AN INVESTIGATION INTO THE IDENTITY OF THE ACTIVE COMPONENT IN PSEUDOCATALASE

By

Neale Wareham

A thesis submitted for the degree of

MASTER OF PHILOSOPHY

UNIVERSITY OF SOUTHAMPTON

Department of Chemistry

February 2002

ACKNOWLEDGMENTS

I would like to thank my supervisor, Professor Geoffrey Luckhurst, for the support and encouragement he has given me over the past years, and for allowing me the use of the facilities at Southampton University. I would also like to thank Dr. Pamela Pedrielli for her help in explaining the finer points of the practical aspects of ESR spectroscopy.

I am grateful to Stiefel Laboratories International R&D for their financial support and to Dr. D. Matkin, Vice-President of Stiefel Laboratories International R&D, for his insight into some of the reaction mechanisms discussed.

Finally, I would like to thank my wife and children for having to bear with the endless calls for peace and quiet during the writing of this thesis.

UNIVERSITY OF SOUTHAMPTON

ABSTRACT

FACULTY OF SCIENCE

CHEMISTRY

Master of Philosophy

An Investigation into the Identity of the Active Component in Pseudocatalase

By Neale Wareham

Pseudocatalase is a potential treatment for the disease Vitiligo (characterised by patchy loss of the pigment melanin in the skin). It has been developed by Professors K. U. Schallreuter and J. M. Woods of Bradford University in collaboration with Stiefel Laboratories International R&D, Maidenhead, UK. It was originally thought that the active moiety of Pseudocatalase was a manganese/bicarbonate complex, which mimics the action of the enzyme catalase in the melanogenesis pathway. This Thesis describes the methods used to try to identify and quantitatively assay the active component. The catalytic activity of Pseudocatalase upon the dye Alizarin, in the presence of hydrogen peroxide, was examined using UV/vis spectroscopy. A capillary electrophoresis method was developed and validated for the assay of manganese EDTA. ESR spectroscopy was used to study the manganese complex in Pseudocatalase. The Thesis also sheds some light on the mode of action of Pseudocatalase in melanogenesis and the role of ethylenediaminetetraacetic acid and bicarbonate in the formation of the active moiety, possibly a bi-nuclear manganese/EDTA/bicarbonate complex.

TABLE OF CONTENTS

Acknowledgements		(i)
Abstract		(ii)
Table of Contents		(iii)
Chapter 1	What is Vitiligo?	
	1.1 Introduction	1
	1.2 The Aetiology of Vitiligo	3
	1.3 Diagnosis	6
	1.4 Treatment	6
	1.5 Pseudocatalase	8
	References	9
Chapter 2	The Catalytic Action of Pseudocatalase	
	2.1 Introduction	11
	2.2 Experimental	14
	2.3 Results	16
	2.4 Discussion	28
	References	30
Chapter 3	Analysis of Manganese EDTA by Capillary Electrophoresis	
	3.1 Introduction	32
	3.2 Development of the Method	37
	3.3 Validation of the Method	45
	3.4 Conclusion	58
	References	60
Chapter 4	Analysis of Manganese EDTA Bicarbonate Complex by ESR	
	4.1 Introduction	62
	4.2 Experimental	68
	4.3 Discussion	81
	References	83
Chapter 5	Conclusions	84
	References	89

Chapter One

What is Vitiligo?

1.1 Introduction

Vitiligo is a skin disease, which causes patchy loss of colour in the skin (hypopigmentation). The patches can be any size and anywhere on the body. They can be large or small but they will always be whiter, not darker than the rest of the skin. The reason for the loss of colour is that the patches lack the skin's natural pigment, melanin, which is produced in specialised skin cells called melanocytes. Vitiligo can also affect the melanocytes in hair follicles, leading to depigmentation of the hair. Unlike hyperpigmentary diseases such as: Addison's disease, Cushing's syndrome and Nelson's syndrome (hormonal related) Vitamin B12 deficiency and cachexia (metabolic disorders). Hyperpigmentation can be drug induced and post-inflammatory, it can also occur in localised patches in conditions such as Melasma.

Fig. 1.1 Photo of Vitiligo in an Indian woman, showing extensive loss of pigmentation.

Vitiligo is a disorder affecting between 0.5 to 4% of the World's population [1, 2], and does not discriminate between race, sex or age although the majority of people develop the disease before they are twenty.

Records of the disease date back many thousands of years, and are mentioned in the "Mahabharata", in Buddhist sacred books, Egyptian pharaonic medicine, and in the Koran and the Bible. However, some of these may have been confused with leprosy which also causes patchy, loss of pigmentation in the skin [3]. Although the disease has been known for such a long time, very little is known as to what causes Vitiligo. There appears to be a consensus that there is a genetic element involved, but that it also requires a "trigger". Inheritance of the gene does not automatically lead to a manifestation of the disease, but rather a predisposition for the disease to develop, subject to some other influence. Known triggers include:

Hormonal changes – Vitiligo may develop during puberty, pregnancy, the menopause or even when taking contraceptives.

Extreme stress – such as bereavement, divorce and redundancy.

Damage to the skin – small cuts and minor sunburn through to major surgery or accidents may trigger the disease.

Other skin conditions such as eczema may damage the skin and also trigger Vitiligo [4].

Vitiligo is not a life threatening disease. It is neither infectious nor contagious. However in most cases, the depigmentation is followed by severe psychological and physical stress [5]. In dark skinned races, where the depigmentation is more noticeable, a large degree of social stigma may be involved. A study on patients with Vitiligo has shown that only a small number adapt to this physical/psychological imbalance [6].

1.2 The Aetiology of Vitiligo

It is quite possible that there is more than one mechanism involved in the appearance of Vitiligo, and that Vitiligo may well be more than one disease. Four theories have so far been proposed: autoimmune, neurogenic, self-destructive and composite; the latter incorporates elements of the other theories [7].

The autoimmune theory suggests that there is an association with other autoimmune disorders such as thyroid disease. The neurogenic theory suggests that melanin production is inhibited by the release of a chemical from the nerve endings in the skin. The self-destructive theory proposes that there is a failure of the normal protective mechanism that removes toxins generated by melanogenesis, thus allowing the toxins to destroy the melanocytes.

It has also been suggested that there may be a genetic aspect to Vitiligo. Studies by Majumder *et al.* [8] and Nath *et al.* [9] seem to indicate that genetic aberrations produce an inclination to develop the disease when aggravated by environmental factors, with the genetic susceptibility requiring more than one gene, possibly three or four being involved.

Although the cause of Vitiligo is still unknown, recent research by Schallreuter *et al.* [10, 11, 12, 17] has found a low activity of the enzyme catalase and an increase of hydrogen peroxide in the skin of Vitiligo patients. It has been suggested that keratinocytes in Vitiligo are unable to recycle 5,6,7,8 tetrahydrobiopterin (6-BH4), an essential cofactor in the hydroxylation of phenylalanine to tyrosine (see Fig. 1.2).

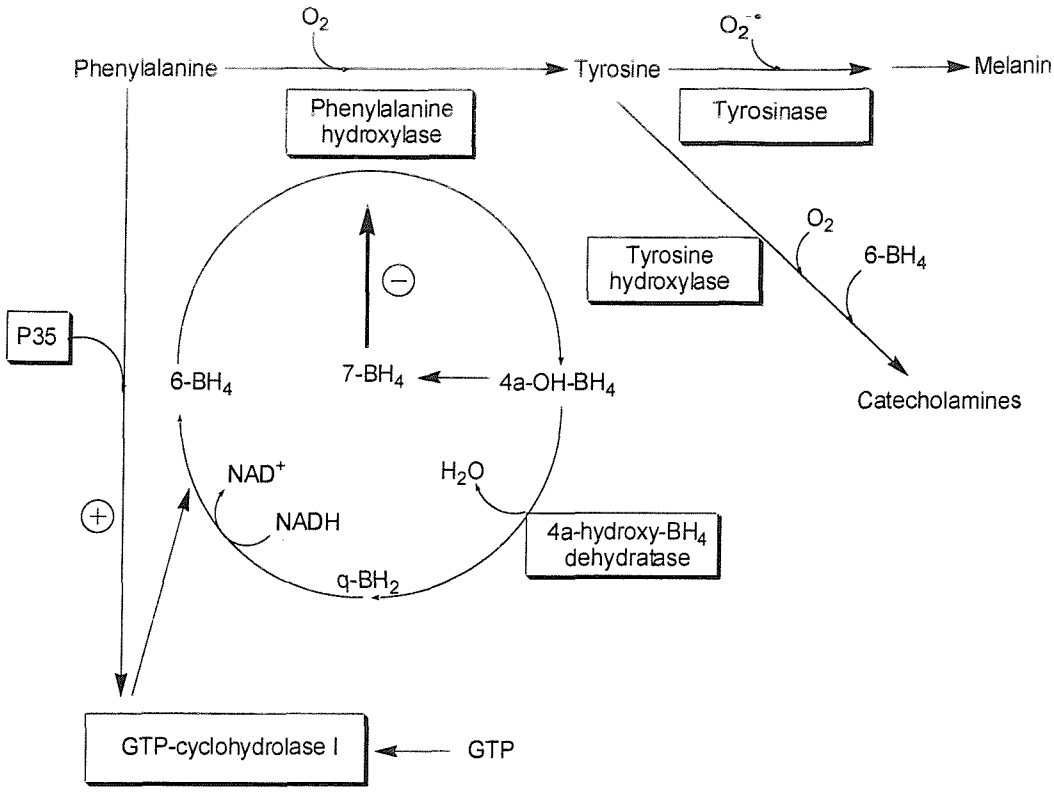

Fig 1.2. Scheme of synthesis and recycling of 6-BH4 in the regulation of tyrosine production by phenylalanine hydroxylase in the epidermis [12, 16].

In Vitiligo, the low activity of 4a-hydroxy-BH4 dehydratase leads to a build up of 7-BH4. Therefore, phenylalanine hydroxylase is inhibited. Phenylalanine accumulates and, by way of a feedback regulator, P35, induces GTP-cyclohydrolase 1. This latter enzyme is the rate limiting step for 6-BH4 synthesis and hence more 7-BH4 is produced causing depigmentation.

This also disrupts the supply of tyrosine to the melanocytes for the production of melanin as shown in Fig. 1.3 resulting in a build up of H_2O_2/O_2^- thus damaging the melanocytes and further disrupting the production of melanin. In this scheme tyrosinase has the unusual property of catalysing three distinct reactions in a single metabolic pathway: the hydroxylation of tyrosine, the dehydrogenation of DOPA and the dehydrogenation of dihydroxyindole (DHI), which, is highly toxic to cells with tyrosinase activity.

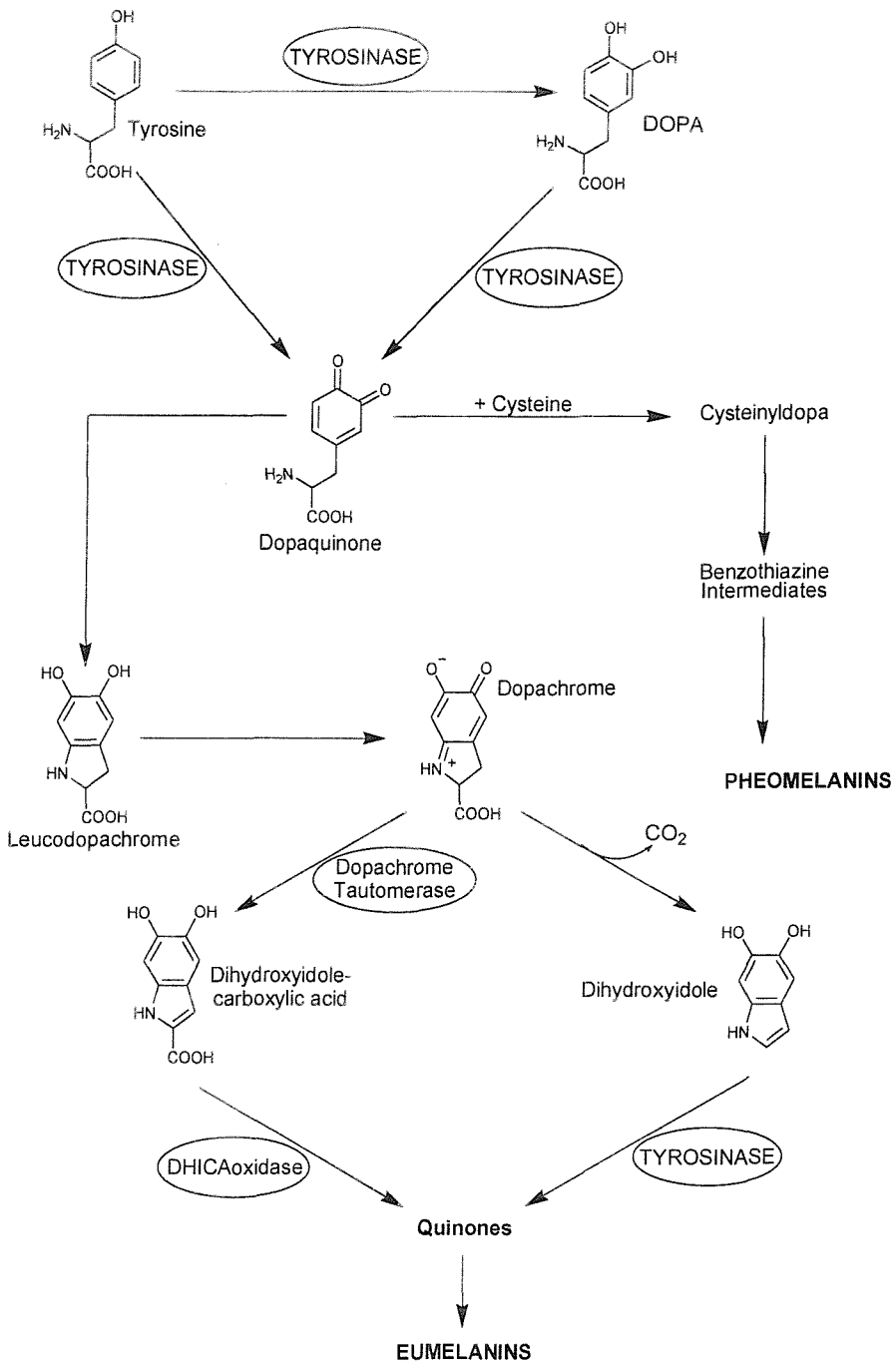

Fig 1.3. The melanin biosynthetic pathway, showing the role of tyrosinase in the formation of both eumelanin and pheomelanin. Eumelanins are the black to dark brown insoluble pigment typically found in human skin and hair. Pheomelanins are yellow to redish-brown, alkali-soluble pigments found almost exclusively in hair, and are formed in the presence of sulphydryl groups [14].

1.3 Diagnosis [13]

The clinical hallmark of Vitiligo is patches of reduced or absent pigmentation giving rise to very white skin. This is usually in a strikingly symmetrical pattern on both sides of the body. There is often a family member who is similarly affected or a relative with other autoimmune diseases such as diabetes and thyroid disease.

Since depigmentation is a gradual process, the early stages of Vitiligo may appear as patches of reduced rather than absent colour. At this stage, it can be difficult to make a definite diagnosis and other clinical factors need to be taken into consideration. These include

a. other causes of reduced pigmentation (e.g. eczema, psoriasis and pityriasis versicolor),

b. observation of the progression of pigment change – to further pigment loss (in Vitiligo) or to return to normal pigmentation (in post inflammatory hypopigmentation).

Rarely, Vitiligo can be confused with uncommon birthmarks or genetic disorders in which loss of pigment is a feature, such as albinism, piebaldism, incontinentia pigmenti and Waardenburg syndrome.

1.4 Treatment [14]

The treatment of Vitiligo can be very difficult and lengthy, and there is a risk of relapse at the end of the course of treatment. In some patients spontaneous repigmentation may occur, which can make it difficult to assess the effectiveness of a course of treatment. In all forms of treatment, the patient must use a high protection factor (15-25) sunscreen as the depigmented areas of skin are highly susceptible to photodamage and the hazards associated with over exposure to ultra violet light.

There are many forms of treatment available to the Vitiligo sufferer. Some of these are purely cosmetic, that is a means to hide the symptoms, such as:

Cosmetic camouflage There is a good range of preparations available, although application can be time consuming and needs to be reapplied daily. Some preparations can rub-off on clothing.

Fake Tans These are similar to cosmetic camouflage, although the active ingredient (usually dihydroxyacetone) chemically binds to the skin. The colour can be built up over a period of days, but then disappears over a similar period after application stops.

Depigmentation For widespread Vitiligo, it is possible to reduce the contrast of light to dark patches by depigmenting the few remaining areas of healthy skin. A monobenzyl ether derivative of hydroquinone is used, however this can cause irritation, contact dermatitis and in rare cases ochronosis (degeneration of the dermal connective tissue). Repigmentation is possible once treatment stops.

Topical Corticosteroids Preparations such as Betnovate (betamethasone valerate) and Dermovate (clobetasol propionate) have been effective for small patches of Vitiligo of recent onset. As with all steroids, follow-up visits to a physician are required to ensure side effects (acne, stretch marks, atrophy etc.) do not occur.

PUVA This is a combination treatment consisting of oral administration of 8-methoxypsoralen (8-MOP) taken two hours before exposure to UVA light (315-400nm). If side effects occur with 8-MOP, then 5-MOP is sometimes used (less side effects, but not as effective). Pigmentation gradually develops in a perifollicular fashion, although it has been known to develop evenly over the whole area. If there is no evidence of a response after three months then treatment is stopped. To avoid risk of photodamage to the skin (reduced chance of skin cancers) treatment is stopped between 100-150 total treatments for white skinned individuals. Only about 30% of patients on PUVA therapy achieve good repigmentation, and of those about 75% will relapse within 2-3 years.

Other Therapies In extreme cases surgical therapies may be considered. These include tattooing, grafting of healthy skin onto the affected area and grafting of cultured melanocytes onto the Vitiligous lesion.

1.5 Pseudocatalase

Pseudocatalase is a potential new treatment for Vitiligo (currently undergoing clinical trials); it has been formulated to act as a substitute for the enzyme catalase in a topical application [15]. The formulation contains a mixture of manganese (II) ions, sodium bicarbonate (in molar excess) and calcium (II) ions, presented in an oil-in-water emulsion or cream. The cream contains mineral oil, white petrolatum, emulsifiers and preservatives. Preliminary trials with this product, when used in conjunction with low dose UVB phototherapy, have shown encouraging results – and that without the phototherapy, application of Pseudocatalase alone, seems to have no clinical effect [15, 17, 18]. However, if Pseudocatalase is to be produced and marketed as a medicinal product then full-scale clinical trials will need to be conducted.

For a clinical trial to take place, the product in question must satisfy certain conditions as defined by the various regulatory authorities. These conditions are primarily directed at ensuring the safety of the patients involved in the trial and include the following:

- identification of the drug substance,
- stability of the drug/product on storage - are there any interactions between the drug and excipients/packaging?
- toxicology – if impurities or degradation products are present do they pose any potential hazards to health?

The research described in this Thesis is directed to help provide some of the answers required for a full-scale clinical trial to proceed. It aims to try to identify the pharmacologically active component of Pseudocatalase and, to develop a stability indicating assay method to provide data in support of registration and licensing of a marketable product.

References

1. J. P. Ortonne, D. B. Mosher, T. B. Fitzpatrick. Vitiligo and Other Hypomelanoses of Hair and Skin. New York, Plenum Press, 1983, p257-258.
2. K. U. Schallreuter, C. Levenig, J. Berger. *Dermatologica.* **183,** 239-245, (1991).
3. M. Lesage. Vitiligo: Understanding the loss of skin colour. The Vitiligo Society 1997, p9.
4. M. Lesage. Vitiligo: Understanding the loss of skin colour. The Vitiligo Society 1997, p10.
5. J. J. Nordlund, A. B. Lerner. *Arch Dermatol.* **118**, 5-7, (1982).
6. B. Salzer, K. U. Schallreuter. *Dermatology.* **190,** 109-115, (1995).
7. M. Lesage. Vitiligo: Understanding the loss of skin colour. The Vitiligo Society 1997, p61.
8. P. Majumder, J. J. Nordlund, S. K. Nath. *Arch. Dermatol.* **129**, 994-998, (1993).
9. S. K. Nath, P. Majumder, J. J. Nordlund. *Am. J. Hum. Genet.* **55**, 981-990, (1994).
10. K. U. Schallreuter, J. M. Wood, M. R. Pittelkow, M. Gütlich, K. R. Lemke, W. Rödl, N. N. Swanson, K. Hitzemann, I. Ziegler. *Science.* **263**, 1444-1446 (1994).
11. K. U. Schallreuter, J. M Wood, M. R. Pittelkow, M. Gütlich, K. R. Lemke, I. Ziegler. *Biochim. Biophys. Acta.* **1226**, 181-192 (1994).
12. K. U. Schallreuter, J. M. Wood, J. Berger. *J. Invest. Dermatol.* **48**, 15-19 (1991).
13. M. Lesage. Vitiligo: Understanding the loss of skin colour. The Vitiligo Society 1997, p62.
14. J. J. Nordlund, R. E. Boissy, V. J. Hearing, R. A. King, J. P. Ortonne. The Pigmentary System – Physiology and Pathophysiology. Oxford University Press, New York, 1998, p537-540.
15. K. U. Schallreuter, J. M. Wood, K. R. Lemke, C. Levenig C. *Dermatology.* **190**, 223-229, (1995).

16. K. U. Schallreuter, J. M. Wood, J. Moore, W. D. Beazley, E. M. J. Peters, L. K. Marles, S. C. Behrens-Williams, R. Dummer, R. Blau, B. Thony. *J. Invest. Dermatol.* **116**, 167 (2001).

17. K. U. Schallreuter, J. M. Wood, J. Moore, W. D. Beazley, D. C. Gaze, D. J. Tobin, H. S. Marshall, A. Panske, E. Panzig, N. A. Hibberts. *J. Invest. Dermatol. Symp. Proc.* **4**, 91 (1999)

18. K. U. Schallreuter. *Skin Pharmacol. Appl. Skin. Physiol.* **12**, 132 (1999)

Chapter Two

The catalytic action of Pseudocatalase

2.1 Introduction

Stadtman *et al.* have suggested that the active moiety in Pseudocatalase is a trisbicarbonate complex of manganese (II) [2 - 4]. However, work carried out by Sychev *et al.* [5 – 13] (in aqueous solution) indicates that this is not so and that the active moiety may possibly be manganese (II) bicarbonate, $Mn(HCO_3)_2$, or a manganese (II) hydrogen carbonate cation, $Mn(HCO_3)^+$.

In one of the experiments conducted by Sychev and his colleagues the catalytic oxidation of the dye Alizarin S (1,2-dihydroxyanthraquinone sulphonic acid), was monitored spectrophotometrically. This compound is of particular interest as it is analogous to L-DOPA, which is present in the melanogenesis pathway (Fig 2.1).

Fig.2.1. Conversion of DOPA to DOPA quinone by the enzyme catalase

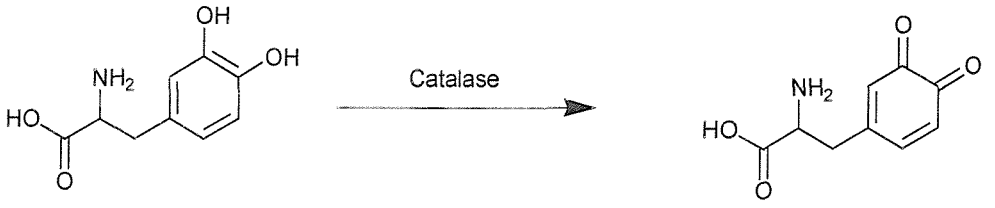

DOPA DOPA Quinone

Fig.2.2. Catalytic oxidation of Alizarin to its quinone by hydrogen peroxide

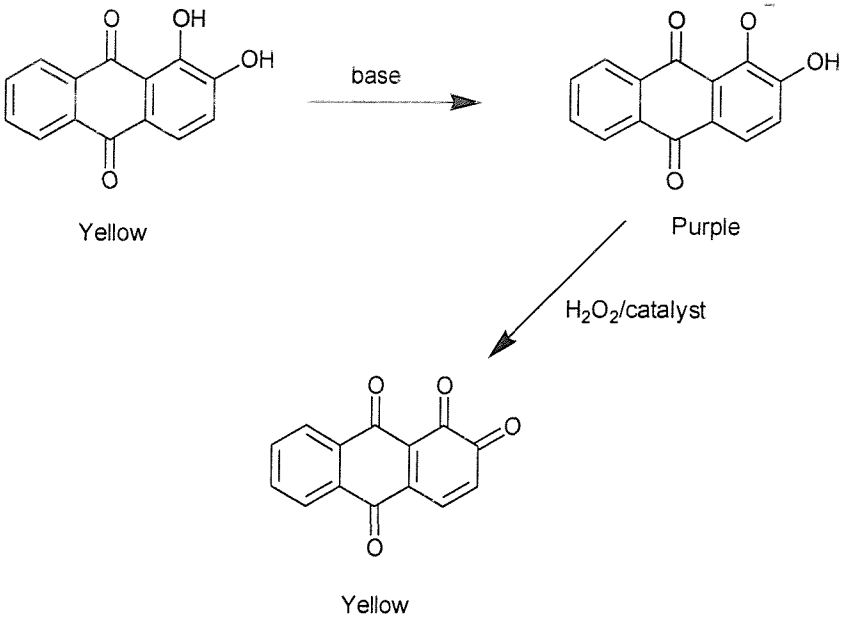

One of the crucial steps in the involvement of Pseudocatalase in Vitiligo is thought to be the prevention of the build up of hydrogen peroxide and the subsequent conversion of tyrosine to dopa-chrome via L-DOPA and DOPA quinone [19]. This is further transformed in subsequent steps to the skin pigment melanin. Alizarin has a very significant structural similarity to L-DOPA, as it also has an ortho-quinol group and it is the reaction of this functional group which is important in the production of melanin from L-DOPA.

The unoxidised dye (in the presence of base) has a purple colour because of extensive delocalisation of π-electrons through the three-ring system and the subsequent negative charge on the O^- groups. When the dye is oxidised by hydrogen peroxide (catalysed by Pseudocatalase,) it is also converted to an o-quinone, which in this case is pale yellow (Fig.2.2). It is concluded that Alizarin may be used as a suitable model for measuring Pseudocatalase activity as it appears to mimic the natural biochemistry (the conversion of an ortho-quinol to an o-quinone). It should be noted at this stage that this is an *in vitro* model and, as with all models, may not reflect fully the processes that occur *in vivo*.

As previously suggested, the active component of Pseudocatalase may be $[Mn(HCO_3)_3]^-$ and is formed in the presence of a molar excess of sodium bicarbonate. The initial preparation of the treatment, used in the preliminary clinical trials involved taking 0.14g of $CaCl_2.2H_2O$ and 0.38g $MnCl_2.4H_2O$ in 3.0ml of

water. To this was added 2.3g of $NaHCO_3$, and the mixture allowed to react. After the effervescence (caused by evolution of CO_2) has ceased 100g of a cream base was added and the resultant product was then used by the patient. Calcium is included in the product as Schallreuter *et al.* have suggested that melanocytes and keratinocytes, in Vitiligous skin, have abnormally low levels of intracellular calcium.

It was noticed that during this reaction a pale pink precipitate was formed, this was assumed to be manganese carbonate, $MnCO_3$. This was confirmed by performing the initial reaction (prior to the addition of the cream base) in the absence of calcium chloride. The resulting precipitate was filtered and washed with water followed by methanol before being sent to an external laboratory for analysis by ICP and AA spectroscopy. The results of this analysis confirmed that the precipitate was $MnCO_3$ (data not shown). This raises the question is the manganese present totally in the form of $MnCO_3$ or is there another manganese compound present, which may be responsible for the observed catalytic activity?

The supernatant fluid from the above reaction was analysed for Mn^{2+} content using an in-house HPLC method (Stiefel ref. AM545 – ion-exchange chromatography with indirect UV detection). The sample was prepared by taking 2ml of solution into a 5ml volumetric flask, conc. HCl was added dropwise until all effervescence had ceased, the solution was the diluted to volume with water before being analysed. (Any manganese compounds present in solution should react with the acid to give $MnCl_2$ in solution – which can then be detected as Mn^{2+}). The results of this analysis indicated that no manganese is present in the solution implying that $MnCO_3$ is the only product of this reaction.

In the experiment conducted by Sychev *et al.* [8], Alizarin S was used as the substrate for the reaction. As Pseudocatalase is in a cream base, it was decided to use Alizarin B (1,2-dihydroxyanthraquinone) and perform the reactions in an organic/water solvent system. This was done as it was thought that a reasonably high organic content would help to break down the physical structure of the cream by disrupting the emulsion of oil and water in the cream, and thus generate results that would be more reliable.

2.2 Experimental

The method developed was as follows:

1.0g of sample was diluted in 100ml of 70:30 methanol/water, shaken and filtered (0.2μm nylon syringe filter). 2.5ml of the filtrate was diluted with 2.5 ml of 70:30 methanol/water. 1.0ml of this solution was pipetted into a standard 1cm glass cuvette, 1.0ml of Alizarin solution (0.2mg/ml in methanol) was added followed by 1.0ml of H_2O_2 solution (0.5 volume in methanol) and the change in absorbance monitored at 530nm.

In this procedure the dye is added before the peroxide solution so as to minimise any effects that may occur due to the peroxide being oxidised by the manganese complex before the dye is added.

It was also considered necessary to confirm Beer's law for the dye used in the experiment as a non-linear response could complicate any rate measurements made and lead to erroneous results.

Solutions of Alizarin B were prepared ranging from 0 to 40mg/100ml. The solutions were used as described in the method, with the exception that the peroxide solution was replaced by 1ml methanol (so no oxidation of the dye occurs during measurement). The absorbance was read at 530nm and the data presented graphically (Fig. 2.3), linear regression analysis of the data gave a regression coefficient of 0.9999. This indicates that the concentration of Alizarin B is proportional to the absorbance over the range examined.

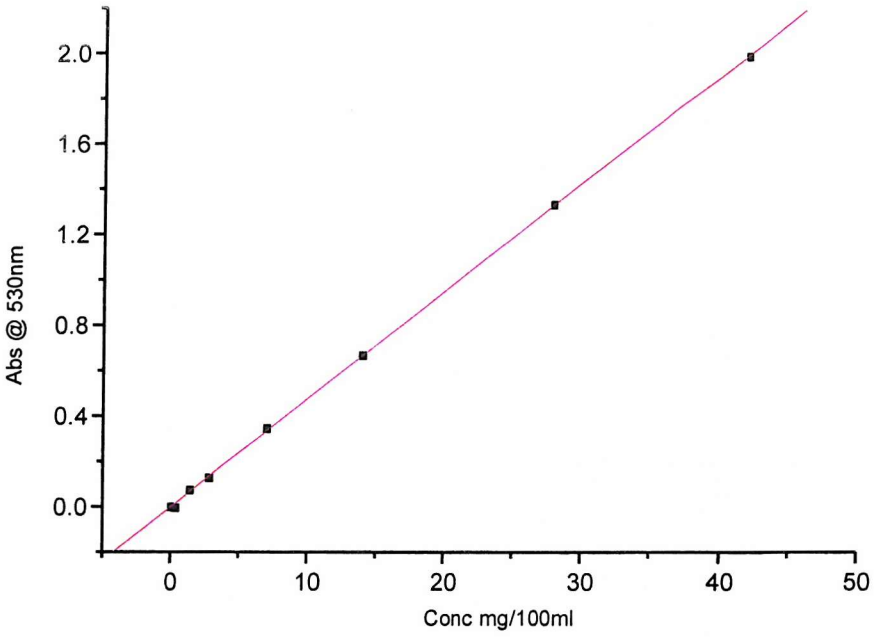

Fig. 2.3. Confirmation of Beer's Law for the dye Alizarin B.

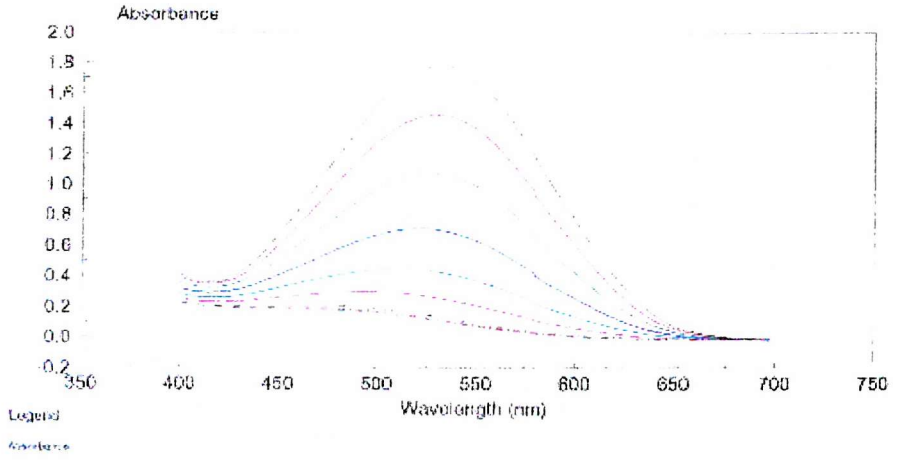

Fig. 2.4 Typical spectra of Alizarin B

Fig. 2.4 shows the peak maximum at 530nm and the decrease in intensity of the absorption peak of Alizarin B with time. The solution was prepared as described in the method and the scans were recorded at approximately 30 s intervals.

2.3 Results

Analysis of Pseudocatalase cream samples.

Multiple analysis of a Pseudocatalase cream sample (single sample analysed six times, n=6) gave typical relative standard deviations (rsd) of 7 to 10%. As this proved to be rather disappointing, it was decided to try to improve the precision of the method, by adding more bicarbonate to the reaction system. It is possible that the amount of bicarbonate in the Pseudocatalase cream samples is not consistent due to the presence of calcium (precipitating as calcium carbonate). To try and overcome this a sample solvent of 70:30 methanol:water that was saturated with sodium bicarbonate was used. In addition, the dye solution was prepared by taking 20mg of the dye adding 50ml of methanol and dissolving. This solution was then made up to 100ml with the bicarbonate saturated methanol/water solution. Using this adaptation of the method, it was possible to improve the precision of the method, and rsd of less than 4% were achieved.

To further reinforce the suggestion that the oxidation of Alizarin may be a suitable model for the conversion of DOPA to DOPA quinone, four other anthraquinone dyes (see Table 2.1) were examined, in place of Alizarin. These results indicate that the ortho positioning of the hydroxyl groups is essential for optimum oxidation of the dye by hydrogen peroxide.

Substrate	Initial abs	Abs at 5min	Δ abs/min
1,2 dihydroxyanthraqinone (Alizarin)	1.90	0.20	0.34
1,4 dihydroxyanthraqinone	1.75	1.40	0.07
1,5 dihydroxyanthraqinone	0.25	0.25	0.00
1,8 dihydroxyanthraqinone	3.00	2.95	0.01
2,6 dihydroxyanthraqinone	0.60	0.60	0.00

Table 2.1. Rate of oxidation of hydroxyanthraquinones.

During this early stage of development of the product, it was noticed that the cream base was not physically stable. The emulsion was starting to break down, forming two distinct layers in the cream. This was probably because the high concentrations

of ionic components disturb the balance of the emulsifiers in the cream. Because of this, the cream base was reformulated with different levels of emulsifiers.

Samples of the new cream formulation were then tested for catalytic activity using the developed method. Surprisingly none of these samples showed any evidence of oxidising the dye. Closer examination of the cream formulations showed that the only difference (apart from the levels of emulsifiers) was that the new formulation did not contain Na_2EDTA, present in the original formulation at 0.1% w/w.

Na_2EDTA is often added to pharmaceutical and cosmetic preparations to improve the physical stability since it forms chelates with free metal ions, which may be present as impurities in the other excipients, in the formulation. Many of the emulsifiers used are anionic (e.g. sodium dodecyl sulphonate) and can ion-pair with cations in the product and thus reduce their effectiveness as emulsifiers.

This raises the question that if Na_2EDTA is essential for the product to show any catalytic activity, then, is there an optimum concentration of Na_2EDTA required in the formulation for it to shows the best activity?

A series of creams were made containing various amounts of Na_2EDTA (the concentrations of manganese, calcium and bicarbonate were kept constant), these were then tested for catalytic activity. The rate of the reaction was determined by monitoring the change in absorbance at 530nm, and calculating the rate of change of absorbance per second (expressed as absorbance units, AU, per second) from the steepest point on the curve, see Fig. 2.5.

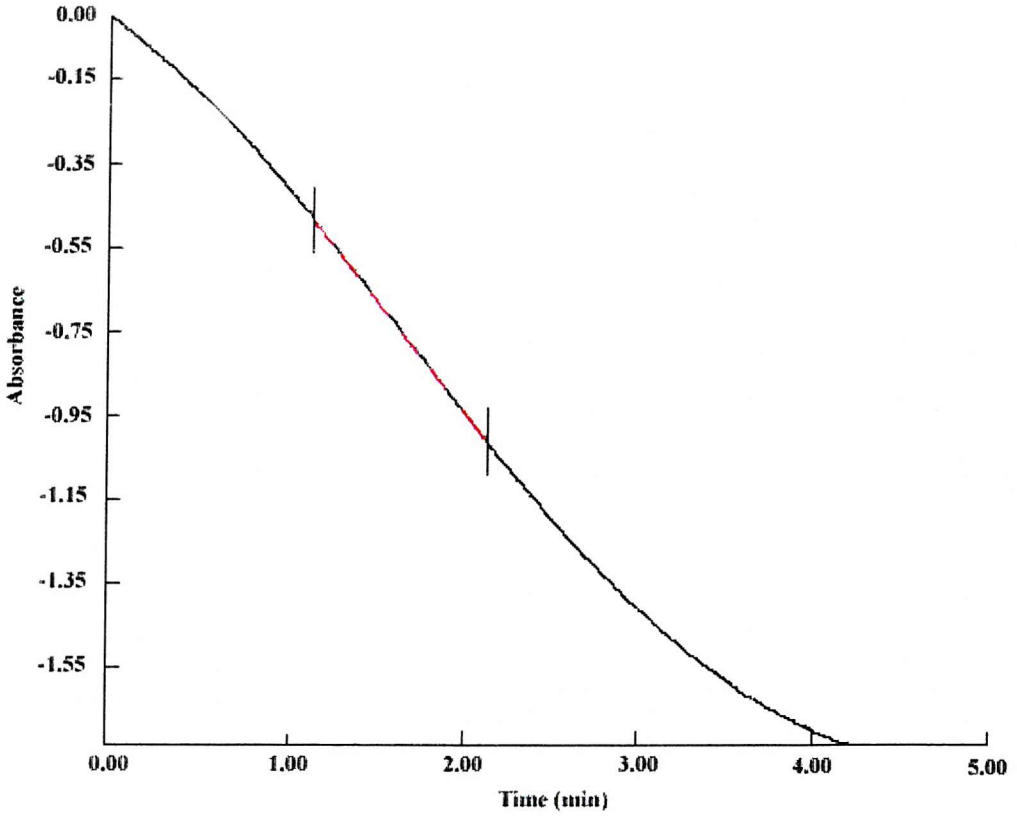

Fig. 2.5. Typical change of absorbance curve against time.

The data obtained for the different Na_2EDTA concentrations are shown in Table 2.2 and Fig 2.6. As can be seen from this data the rate of reaction is at a maximum when the Na_2EDTA concentration is about 0.6% w/w. This corresponds approximately to a 1:1 molar ratio with manganese.

%w/w Na_2EDTA	0	0.02	0.05	0.1	0.3	0.5	0.7	1.0	1.2	1.4	1.6
Rate $x10^{-5}$ AUs^{-1}	12	130	232	328	434	481	468	372	4	3	2

Table 2.2. Effect of Na_2EDTA concentration upon the rate of reaction.

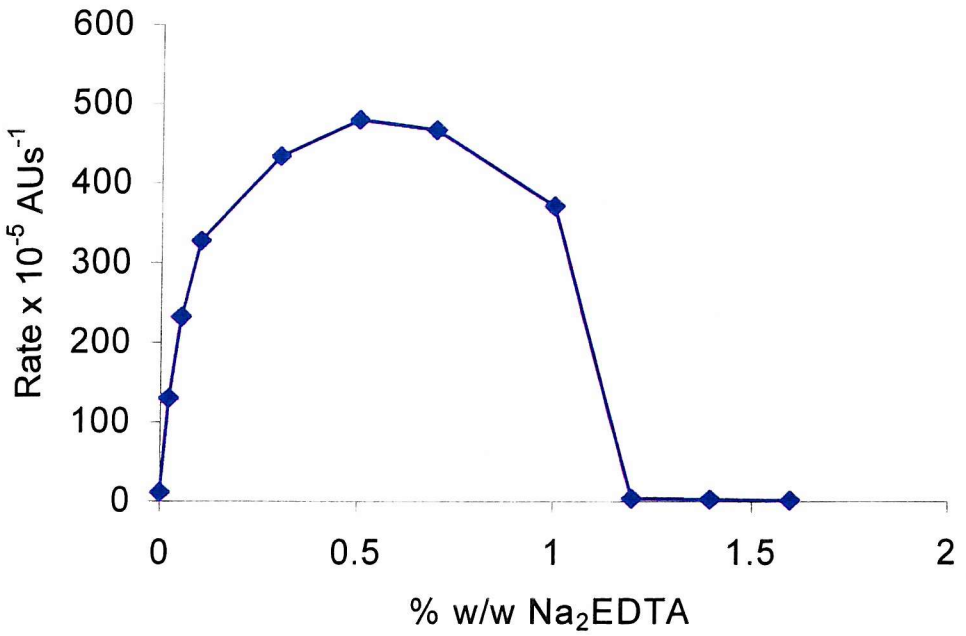

Fig. 2.6. Effect of Na_2EDTA concentration upon reaction rate.

The shape of the curve is somewhat unexpected, it was originally thought that the rate would increase with concentration, to an optimum level, and then remain constant. However, this data indicates that too high a concentration of Na_2EDTA can reduce the catalytic activity. It is possible that when excess Na_2EDTA is added, the bicarbonate is driven off the complex forming the non-active MnEDTA.

As a result of this information the cream formulation was further modified to incorporate an Na_2EDTA level of 0.5% w/w. Although this is not the optimum concentration of Na_2EDTA it is the maximum permissible amount (from the various regulatory authorities) that can be incorporated into a pharmaceutical product.

To investigate the effects of changing the concentration of the various active components (manganese and bicarbonate), further experiments were conducted on cream samples containing:

1. A range of manganese concentrations (Na_2EDTA, calcium and bicarbonate constant at 0.5 and 2.3% w/w respectively).

2. A range of bicarbonate concentrations (Na_2EDTA, calcium and manganese constant at 0.5 and 0.38% respectively).

These data are summarised in Tables 2.3 and 2.4 and Figs. 2.7 and 2.8

Fig. 2.7 demonstrates the change in reaction rate with the change in manganese concentration. As expected, the rate initially increases as the concentration of manganese increases until it reaches a plateau region where the rate levels off and remains almost constant irrespective of any further increase in manganese. The point at which the rate ceases to change is equivalent to the manganese added reacting with all the available Na_2EDTA, any further addition of manganese will only react with the bicarbonate to form $MnCO_3$, hence no further change in activity.

Manganese concentration (as % of nominal)	Manganese concentration (as µg/ml)	Rate x 10^{-5} AU.s^{-1}
0	0	0
1	0.345	3
2	0.721	5
4	1.455	9
10	3.901	28
15	5.583	42
20	8.093	65
40	14.240	100
60	20.814	115
80	29.256	122
100	37.083	125
120	44.700	125

Table 2.3. Variation of rate with changing manganese concentration.

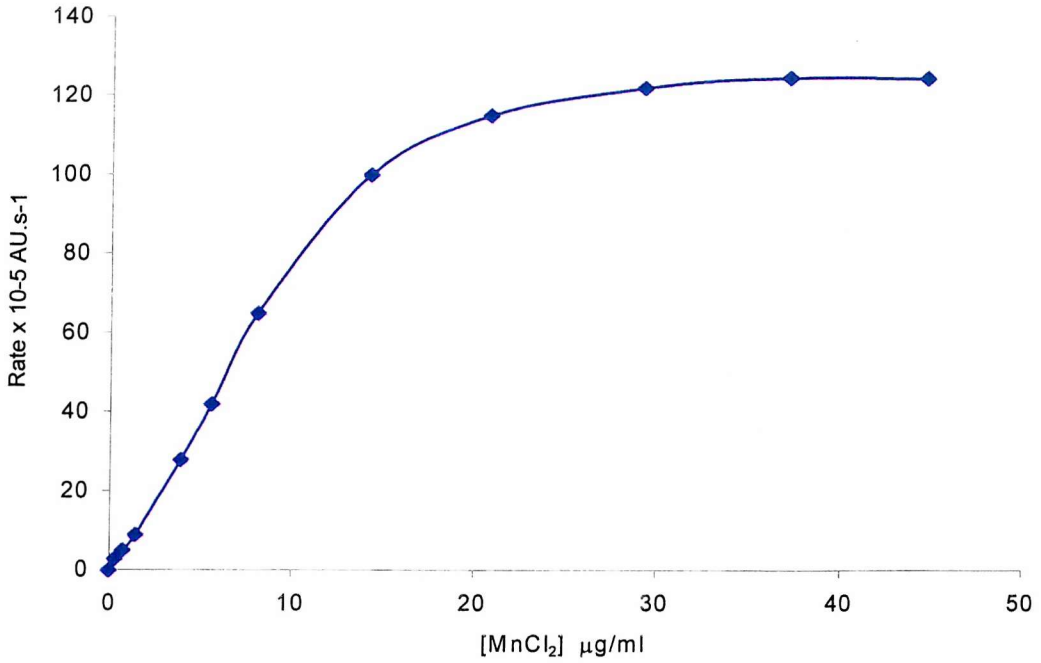

Fig. 2.7. Variation of rate with changing manganese concentration.

Bicarbonate concentration (% w/w)	ln(bicarbonate concentration)	Rate x 10^{-5} AU.s^{-1}
0	-	0
0.01	-4.61	20
0.025	-3.69	80
0.05	-3.00	140
0.1	-2.30	197
0.25	-1.39	250

Table 2.4. Variation of rate with changing bicarbonate concentration.

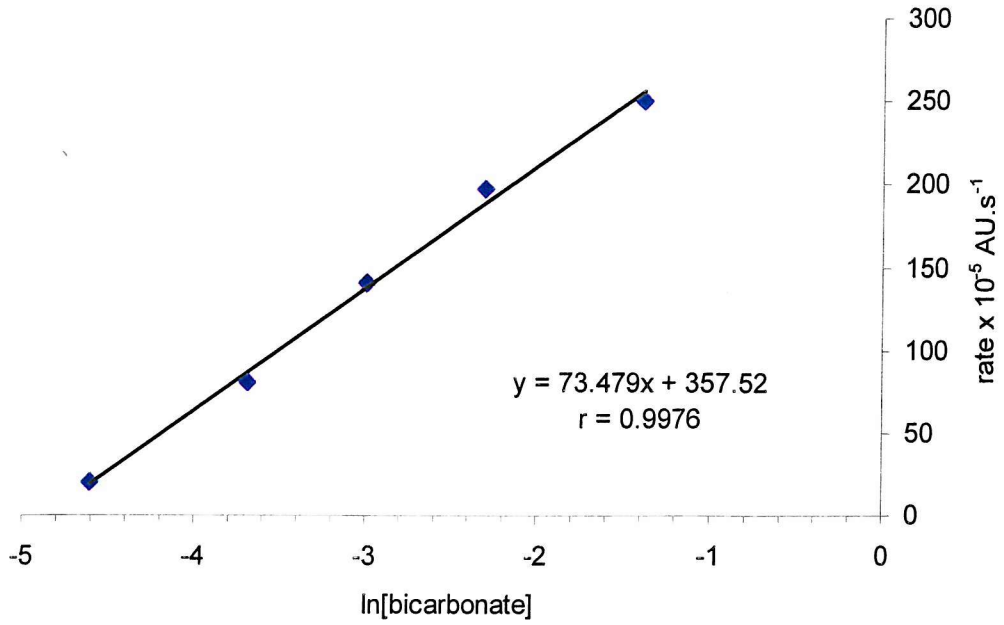

Fig. 2.8. Variation of rate with changing bicarbonate concentration.

Fig 2.8 clearly demonstrates that the rate of reaction is first order with respect to bicarbonate concentration As can be seen from this data, manganese, Na_2EDTA and bicarbonate are essential for the cream to show any catalytic activity. If any one of the three components is missing then no activity is observed.

A possible explanation for this is that EDTA can react with the solid manganese carbonate (formed from the mixing of manganese chloride and sodium bicarbonate) to give a manganese (II) EDTA complex. The large excess of bicarbonate may possibly displace one or more of the carboxylic groups of the EDTA molecule; hence the active catalyst could well be a manganese/EDTA/bicarbonate complex. A possible mechanism for this is given in Fig. 2.9.

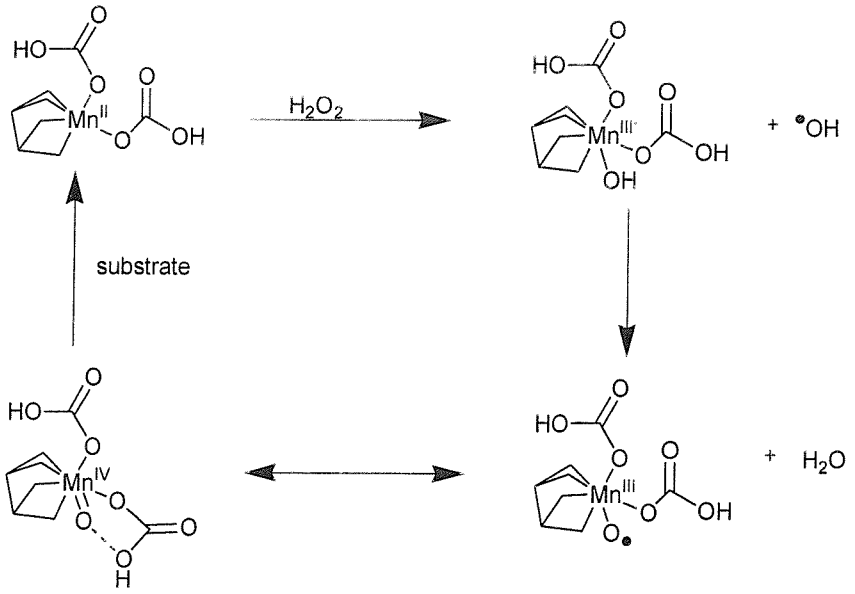

Fig. 2.9. Possible mechanism for the formation of a manganese (IV) oxinoid species responsible for the oxidation of a substrate (Alizarin) and subsequent regeneration of the manganese (II) complex.

In Fig. 2.9 the manganese/bicarbonate/EDTA complex reacts with peroxide to give a hydroxylated Mn^{III} intermediate and a hydroxyl radical, the hydroxyl radical then reacts with the hydroxylated Mn^{III} intermediate and extracts the H^+ to give a Mn complex radical. This undergoes internal rearrangement to produce the Mn^{IV} oxinoid species that can then oxidise the substrate.

At this point in the investigation, it was decided to see if other complexing agents, apart from Na_2EDTA would act in a similar way. It was decided to see whether EDTA type analogues would behave in a similar manner to Na_2EDTA. Several other common complexing agents were also tested (readily available from laboratory stock).

Samples of cream were prepared containing different complexing agents, at a 1:1 molar ratio with manganese. The creams were tested for catalytic activity as described previously, and the results tabulated relative to the activity of the cream sample containing Na_2EDTA, see Table 2.5.

Chelating Agent	Rate x 10^{-5} AU.s^{-1}	Relative rate
Na_2EDTA	236	1.0
Na_4EDTA	**239**	**1.0**
H_4EDTA	**245**	**1.0**
1,3 diaminopropanetetraacetic acid (1,3-DPTA)	145	0.6
1,2 diaminopropanetetraacetic acid (1,2-DPTA)	66	0.3
2-hydroxyethylethylenediaminetriacetic acid (HEDTA)	**302**	**1.3**
Ethyleneglycol(aminoethyl)tetraacetic acid (EGTA)	**410**	**1.7**
Diethylenetriaminepentaacetic acid (DTPA)	**242**	**1.0**
Triethylenetetraaminehexaacetic acid (TTHA)	**301**	**1.3**
Diaminocyclohexanetetraacetic acid (DCTA)	24	0.1
Diaminohexanetetraacetic acid (DHTA)	8	0.0
Ethylenediaminetetrapropionic acid (EDTPA)	26	0.1
8-hydroxyquinoline-5-sulphonic acid	59	0.2
1-(2-pyridylazo)-2-naphthol	31	0.1
4-(2-pyridylazo)resorcinol (PAR)	**709**	**3.0**
4-(4-nitrophenylazo)resorcinol	9	0.0
2,6-pyridinedicarboxylic acid	**119**	**2.0**
1,10-phenanthroline	26	0.1
Ascorbic acid	7	0.0
Citric acid	**294**	**1.25**
Tartaric acid	5	0.0
Oxalic acid	5	0.0
Salicylic acid	8	0.0

Table 2.5. Activity of other chelating agents w.r.t. Na_2EDTA. Chelating agents in bold show an activity equivalent to, or greater than Na_2EDTA.

This data demonstrates that, as could be reasonable expected, several EDTA analogues also show catalytic activity in the presence of manganese and bicarbonate. Little difference was seen between the rates of H_4EDTA, Na_2EDTA and Na_4EDTA, whereas HEDTA, EGTA and TTHA all show increased catalytic activity. Closer examination of the physical data for the EDTA analogues indicates that there is a linear relationship between the relative activity and the absolute stability constants of the chelating agents ($logK_1$) with Mn^{II} [14, 15] as shown in Table 2.6 and Fig 2.10.

Chelating Agent	Absolute stability constant ($logK_1$)
Na_2EDTA	14.0
Diaminocyclohexanetetraacetic acid (DCTA)	16.8
Ethyleneglycol(aminoethyl)tetraacetic acid (EGTA)	12.3
Diethylenetriaminepentaacetic acid (DTPA)	15.5
Triethylenetetraaminehexaacetic acid (TTHA)	14.6
4-(2-pyridylazo)resorcinol (PAR)	9.8

Table 2.6. Stability constants for the formation of manganese complexes of some of the chelating agents used.

It was noted that citric acid, 4-(2-pyridylazo)resorcinol and 2,6-pyridinedicarboxylic acid also showed an increase in catalytic activity, although the reason for this is not clear.

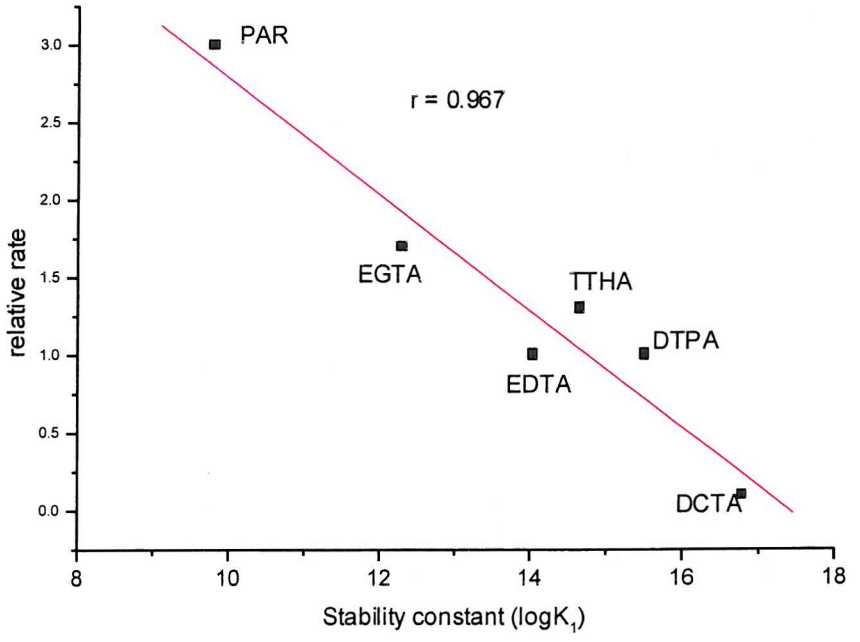

Fig. 2.10. Relationship between chelating agents and catalytic activity.

This data appear to confirm the proposal that an excess of bicarbonate can displace one or more of the metal-chelate bonds to form a metal/chelate/bicarbonate complex. The larger the stability constant, the stronger the bonds between the metal and the chelate. Thus, for the weaker complexes, it is easier for bicarbonate to displace one

of the metal-chelate bonds and form more of the active metal/chelate/bicarbonate complex.

During the analysis (using the Alizarin dye method) of Pseudocatalase cream samples and the stability assays, which were also taking place, it became apparent that there was a major problem with the method. Although the intra-day (analysis of samples performed on the same day) precision of the method was reasonable good, with rsds < 5% on repeat samples; the day to day reproducibility was extremely poor. Variations of +/- 50% on the rate measurements have been observed for the same batch of product analysed on different days. Stadtman *et al.* [2] have shown that the presence of inorganic phosphate and pyrophosphate can inhibit the catalytic action of the manganese/bicarbonate system. It is possible that, as many commercial laboratory-cleaning agents contain inorganic phosphates, there may be some contamination of the glassware used for these experiments. Tables 2.7 and 2.8 show the data obtained for the analysis of the same batch of Pseudocatalase cream (SF156/05/A). The results were generated from repeat analysis of the same sample on the day of manufacture and after 7 days storage at 25°C.

Batch SF156/05/A	Rate x 10^{-5} $AU.s^{-1}$
Sample 1	558
Sample 2	559
Sample 3	582
Sample 4	537
Sample 5	565
mean	560
% rsd	2.9

Table 2.7. Initial rate data for Pseudocatalase cream – batch SF156/05/A

Batch SF156/05/A	Rate x 10^{-5} AU.s^{-1}
Sample 1	845
Sample 2	892
Sample 3	874
mean	870
% rsd	2.7

Table 2.8. Rate data for Pseudocatalase cream – batch SF156/05/A after 7 days storage at 25°C

At the next time point for this batch (14 days), all glassware and reagent bottles were washed as usual, followed by soaking overnight in 50% nitric acid. The glassware was then rinsed manually with demineralised water and dried before use. The same procedure was used at the 28 day time point for this batch. The results for these analyses were a mean rate of 420 x 10^{-5} AU.s^{-1} at 14 days and 655 x 10^{-5} AU.s^{-1} at 28 days (samples were analysed in triplicate at each time point). This careful washing procedure appears to make no difference to the variability of the results generated.

2.4 Discussion

The results in this Chapter have brought to the fore some interesting information on the nature of the active component in Pseudocatalase cream. What was originally thought to be a relatively simple manganese/bicarbonate complex now appears to be a more intricate system involving manganese/bicarbonate/EDTA. It seems likely that the complex is $[Mn(HCO_3)_2EDTA]^{2-}$, and that several possibilities exist as to how this interacts with both hydrogen peroxide and Alizarin to produce the o-quinone.

1. Both the substrate and peroxide bind to the manganese cation, where the oxidation takes place; a so-called inner-sphere oxidation. However, this seems unlikely given the presence of EDTA, which would need to be displaced to allow the substrate access to the manganese.
2. The manganese is taken to a higher oxidation state such as Mn^{III} or Mn^{IV}, which is then responsible for oxidising the substrate. This would explain the need for the EDTA to stabilise the higher oxidation states, otherwise Mn^{IV} would be precipitated as manganese oxide. Again, the nature of the ligands would seem to prevent this being an inner-sphere oxidation mechanism.
3. The manganese complex could be involved in the production of hydroxyl radicals (outer-sphere oxidation) which then oxidise the substrate.

Although Schallreuter *et al.* [1,16-18] have suggeated that melanocytes and keratinocytes, in Vitiligous skin, have low levels of intracellular calcium, the inclusion of calcium in this formulation is questionable. As, with the quantities of reagents used, and the stability constants for the EDTA complexes of Mn(II) and Ca(II) (the value for Mn^{2+} being three log units greater than that for Ca^{2+}), all the calcium will be present in the form of the insoluble carbonate. Thus, it is unlikely that Ca^{2+} will penetrate through the skin. In addition, no activity is seen if manganese is omitted from the test samples (samples containing calcium, Na_2EDTA and bicarbonate). In hindsight, it is possible that the calcium could have been added separately from the manganese/bicarbonate mixture (as proposed by Schallreuter and Woods). As the order of preparation of the product could affect the activity of the product, although this has not been investigated at this stage.

The method for monitoring the catalytic activity, although irreproducible from day to day, has given some useful information in that it can be used to observe trends in the

reaction process. So far, it has not been possible to determine the cause of the variation in results. It has been shown that careful cleaning of the glassware used for the sample preparation does not alleviate this problem. Another possible cause is that the rate of reaction could be temperature sensitive. The experiments performed by Stadtman and Sychev were all thermostatically controlled. It has not been possible to do this in the laboratory at Stiefel, as the spectrophotometer used for these experiments does not have the capability of controlling temperature in the cell compartment. It is also possible that although the sample solvent was saturated with sodium bicarbonate, the actual concentration of bicarbonate in the supernatant fluid changes as a function of the temperature of the solution. These are factors which could be examined at a later date should the equipment and time become available.

Note: Due to the problems encountered with this method, that it was not possible to generate meaningful stability data, and that there appears to be no correlation between the rate data obtained and the physical characteristics of the cream samples, this method has now been dropped from the analytical protocols for the stability testing of Pseudocatalase cream.

References

1. K. U. Schallreuter, J. M. Wood, K. R. Lemke, C. Levenig. *Dermatology.* **190**, 223, 1995
2. E. R. Stadtman, B. S. Berlett, P. B. Chock. *Proc. Natl. Acad. Sci. USA.* **87**, 384,1990
3. E. R. Stadtman, B. S. Berlett, P. B. Chock. *Proc. Natl. Acad. Sci. USA.* **87**, 389,1990
4. E. R. Stadtman, B. S. Berlett, P. B. Chock. *Proc. Natl. Acad. Sci. USA.* **87**, 394,1990
5. A. Ya Sychev, U. Pfanmeller, V. G. Isak. *Russ. J. Phys. Chem.* **57** (7), 1024, 1983
6. A. Ya Sychev, U. Pfanmeller, V. G. Isak. *Russ. J. Phys. Chem.* **57** (3), 464, 1983
7. A. Ya Sychev, U. Pfanmeller, V. G. Isak. *Russ. J. Phys. Chem.* **57** (8), 1193, 1983
8. A. Ya Sychev, U. Pfanmeller, V. G. Isak. *Russ. J. Phys. Chem.* **57** (8), 1197, 1983
9. A. Ya Sychev, U. Pfanmeller, V. G. Isak. *Russ. J. Phys. Chem.* **57** (9), 1349, 1983
10. A. Ya Sychev, U. Pfanmeller, V. G. Isak. *Russ. J. Phys. Chem.* **59** (7), 1004, 1985
11. A. Ya Sychev, U. Pfanmeller, V. G. Isak. *Russ. J. Phys. Chem.* **58** (4), 549, 1984
12. A. Ya Sychev, U. Pfanmeller, V. G. Isak. *Russ. J. Phys. Chem.* **55** (2), 202, 1981
13. A. Ya Sychev, U. Pfanmeller, V. G. Isak. *Russ. J. Phys. Chem.* **51** (2), 212, 1977
14. R. M. C. Dawson, D. C. Elliott, W. H. Elliott and K. M. Jones, Data for Biochemical Research, 3rd ed., Clarendon Press, Oxford (1986).
15. C R C Handbook of Organic Analytical Reagents (K. L. Cheng, K. Ueno, T. Imamura, eds.), C R C Press, Boca Raton (1982).

16. K. U. Schallreuter, J. M. Wood, J. Moore, W. D. Beazley, E. M. J. Peters, L. K. Marles, S. C. Behrens-Williams, R. Dummer, R. Blau, B. Thony. *J. Invest. Dermatol.* **116**, 167, 2001.

17. K. U. Schallreuter, J. M. Wood, J. Moore, W. D. Beazley, D. C. Gaze, D. J. Tobin, H. S. Marshall, A. Panske, E. Panzig, N. A. Hibberts. *J. Invest. Dermatol. Symp. Proc.* **4**, 91, 1999

18. K. U. Schallreuter. *Skin Pharmacol. Appl. Skin. Physiol.* **12**, 132 (1999)

19. C. J. Cooksey, P. J. Garret, E. J. Land, S. Pavel, C. A. Ramsden, P. A. Riley, N. P. M. Smit. J. Biol. Chem. **272** (42), 26226, 1997

Chapter Three

Analysis of Manganese EDTA by Capillary Electrophoresis

3.1 Introduction

It has been shown in Chapter 2 that Na_2EDTA is required for Pseudocatalase to demonstrate catalytic activity using the Alizarin dye test. Therefore, it is reasonable to assume that any manganese present in the formulation will be present in the form of its chelate. In this Chapter we describe the development of a stability indicating method for the analysis of manganese EDTA. A stability indicating method is defined as a method of sufficient selectivity to be able to detect any changes in the level of analyte in the product being tested. Ideally, it should also be able to detect and quantify any degradation products formed over the period of the stability trial.

There are many liquid chromatographic methods for the analysis of metal EDTA complexes available in the current literature. Most of these are not, however, stability indicating, because many of the methods available tend to use either excess EDTA [1-6] or a competing metal ion in the mobile phase, to form a complex in situ with the metal or chelate of interest [7-10]. While others use ion-pairing reagents[11-14]. Some of these papers have reported problems with ghost peaks and peak splitting much of which has been attributed to disturbances in the equilibrium between the mobile phase, stationary phase and the ion-pair reagent. One of the problems with using EDTA in an HPLC system is that the mobile phase is exposed to a large surface area of metal (stainless steel). This can be in the pump heads, the connecting tubing, and the column itself. Some of the poorer quality silica used as packing material also contain relatively high (up to one percent) quantities of metal impurities. Hence the need for lengthy equilibration periods (typically overnight or up to 24 hours) of the HPLC system before the analysis takes place.

In the past decade several capillary electrophoresis methods have been developed for the analysis of metal ions, chelating agents, and complexes of the two [15-22]. As with the liquid chromatographic methods, many of these use an excess of metal ion

or chelating agent as part of the electrolyte system. However, the separation system is of a simpler nature i.e. the column is made of fused silica capillary. There is no silica support or bonded phases, no need for ion-pair reagents, they can operate over a wider pH range, (typically pH 2-10), and an aqueous based electrolyte/buffer is typically used. In addition, in CE, the detection is usually performed "on-column" (see Fig. 3.1), this means that direct UV detection at wavelengths down to 190nm is easily achieved. This is due to the short pathlength of the detector cell and hence a lower background absorbance.

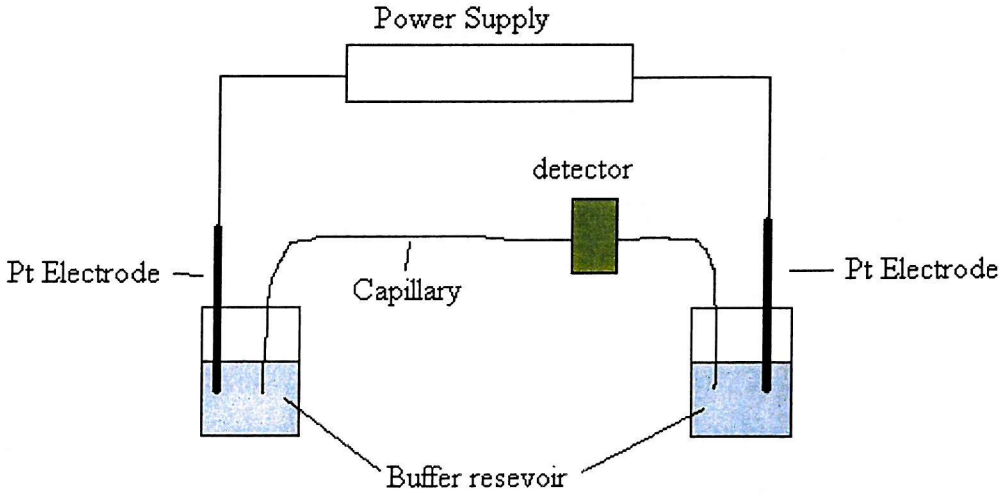

Fig. 3.1 Basic schematic of a CE instrument.

Because detection can be performed at low wavelengths, this technique is ideally suited for the analysis of compounds with no appreciable chromophore such as MnEDTA (see Fig. 3.2)

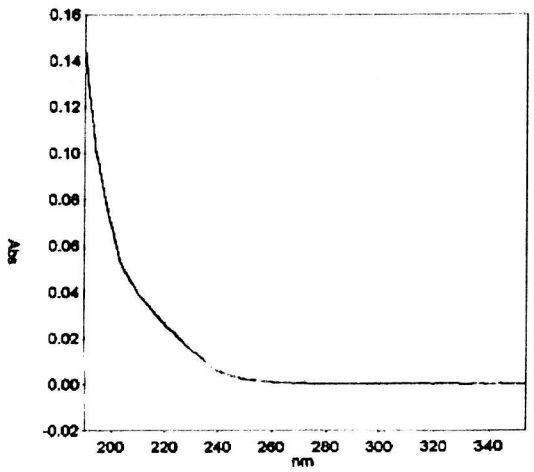

Fig 3.2 UV absorption spectrum of MnEDTA in water.

Capillary Electrophoresis

A century of development in electrophoresis and instrumentation has provided the foundation for capillary electrophoresis. The direct forerunner of this technique has been attributed to Hjerten [22]. Reviews describing the history of electrophoresis have been published by Compton and Brownlee [23] and by Vesterberg [24]. For general information on the theory of electromigration techniques, there is an excellent review by Kleparnik and Bocek [25].

Capillary Electrophoresis can be used in many different modes of separation. These modes include capillary zone electrophoresis (free solution capillary electrophoresis) (CZE or FSCE) and micellar electrokinetic chromatography (MEKC/MECC). In CZE the separation is based purely on the mass and charge of the analyte, while in MEKC surfactants are added to the mobile phase. This gives additional selectivity based on partitioning of the analyte between the buffer and the micelles formed by the surfactant (analogous to the separation mode in reverse phase HPLC). In theory CE in not a complex technique, however some fundamental factors are critical to obtaining a good separation.

pH

In most modes of separation, the analyte molecules are charged, as either weak acids or weak bases; the net charge on the molecule being a function of its pH. Separations of similarly charged analytes can succeed or fail based on a difference as small as 0.2 pH units.

Flow

The pumping mechanism in CE is called electroendoosmosis and provides a narrow 'plug-type' (Fig. 3.3) flow profile through the column (unlike HPLC, which gives a laminar flow profile).

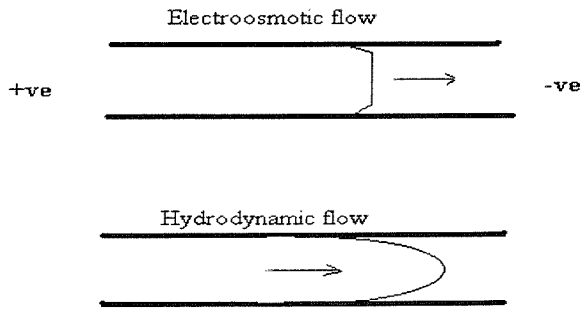

Fig 3.3 Electrically driven and pressure driven capillary flow profiles.

The flow occurs because of the surface charge (*zeta potential*) on the wall of the capillary. With fused silica capillaries, the surface contains ionised silanol ($Si\text{-}O^-$) groups. The negatively charged wall attracts cations from the buffer solution (those closest to the wall are held immobile) whilst those further out form a positively charged layer which is free to move. This diffuse outer region is known as the Gouy-Chapman layer. The rigid inner layer is called the Stern layer (see Fig 3.4).

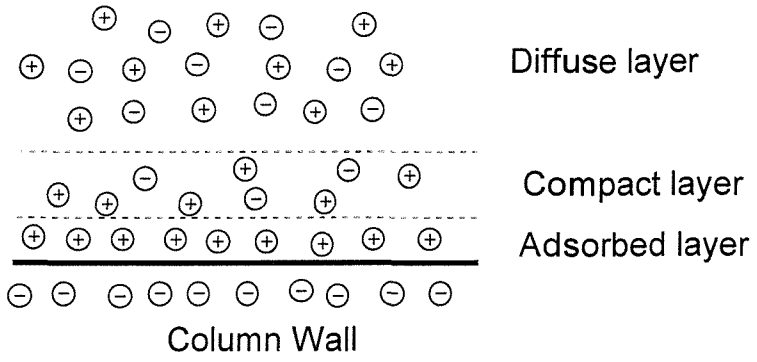

Fig 3.4 Representation of the electrical double layer in a capillary column.

As a voltage is applied, the positive charges move in the direction of the cathode. Since the ions are solvated by water, the fluid in the buffer is mobilised as well and dragged along by the migrating charge. The movement of the buffer along the capillary is called the Electroosmotic Flow (EOF).

Capillary

In CE, the capillary is an integral part of the separation process; its main contribution is the EOF. Changes in the chemistry of the capillary wall can have a marked effect on the EOF and subsequently the migration time of the analytes. In un-coated fused silica capillaries the flow can be directed towards the anode, towards the cathode or held almost stationary just by changing the content of the electrolyte/buffer system. The EOF can be controlled by several methods; these include controlling the pH of the buffer, adding organic solvent to the buffer and the addition of surfactants. In the first case, adjusting the pH will cause the charge (zeta potential) on the capillary wall to change due to the degree of ionisation of the silanol groups. At low pH few silanol groups will be ionised (little or no EOF), at high pH all available silanol groups will be ionised (high EOF).

Organic solvents modify the EOF due to their impact on buffer viscosity [26] and zeta potential (via solvation effects on the buffer ions and increasing the pK_a values of the surface silanol groups) [27]. In general at high pH, increasing organic solvent concentration usually decreases the EOF [27]. Typical solvents used are alcohols (methanol, ethanol, propanol and isopropanol), acetonitrile, acetone, tetrahydrofuran and dimethyl sulphoxide.

Surfactants are used mainly as a pseudophase in MEKC and were first described in 1984 by Terabe [28]. In this technique, surfactants are added at a concentration high enough for the surfactant molecules to aggregate and form micelles. The concentration and degree of aggregation will depend on the type of surfactant used. For sodium dodecyl sulphonate, commonly used in MEKC, the critical micellar concentration (CMC) is 8.2mM and the aggregation number is about 62. However, by using a cationic surfactant at a concentration level below the CMC the direction of the EOF can be reversed [29, 30]. Flow reversal occurs because the cationic "head" of the surfactant is attracted to the negative charge on the capillary wall. The result is a double layer of surfactant molecules which effectively coats the capillary wall with a positive charge and thus reverses the flow of the liquid in the capillary (see Fig. 3.5)

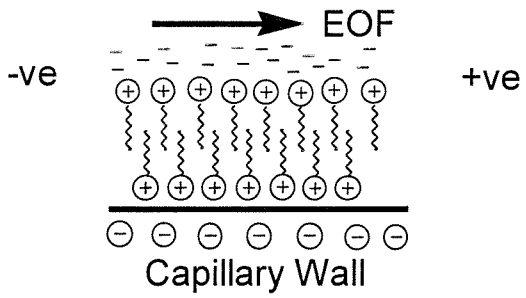

Fig 3.5 Cationic surfactant mediated charge reversal.

3.2 Development of the method

Motomizu *et al.* [31] have described a capillary electrophoresis method for the analysis of alkaline-earth metal EDTA complexes. The method described used 20mM sodium tetraborate (borax) and 2 to 20mM disodiumEDTA in the buffer solution. The EDTA is added to complex in-situ with the metal ions in the sample. As EDTA is added to the buffer this would not be a stability indicating method for a metal EDTA complex. Any free metal in the solution (possibly formed because of dissociation of the complex) would not be distinguished from its bound form. This paper also gives details of the electrophoretic mobility (μ_{ep}) of other divalent metal ions, including manganese, they are

$Ca^{2+} = 3.19 \times 10^{-4}\ cm^2V^{-1}s^{-1}$
$Mg^{2+} = 3.39 \times 10^{-4}\ cm^2V^{-1}s^{-1}$
$Mn^{2+} = 3.86 \times 10^{-4}\ cm^2V^{-1}s^{-1}$
$Co^{2+} = 4.02 \times 10^{-4}\ cm^2V^{-1}s^{-1}$
$Zn^{2+} = 4.04 \times 10^{-4}\ cm^2V^{-1}s^{-1}$
$Cu^{2+} = 4.11 \times 10^{-4}\ cm^2V^{-1}s^{-1}$

These data indicate that using this system separation of the two metal cations present (Ca^{2+} and Mn^{2+}) in the Pseudocatalase formulation is possible. It can also be seen that the mobility of Cu^{2+} is sufficiently different from Ca^{2+} and Mn^{2+} so as to enable it to be considered as a potential internal standard.

At the time of this experiment no sodium tetraborate was available, however it was possible to prepare an equivalent buffer using boric acid and sodium hydroxide (20mM tetraborate, pH 9.5 ~ 80mM boric acid/NaOH, pH 9.5). This buffer was prepared without the addition of any Na_2EDTA. Solutions containing 0.05%w/w each of $Na_2CaEDTA$, $Na_2MnEDTA$ and $Na_2CuEDTA$ was analysed using this buffer system on an uncoated fused silica capillary (50μm i.d.) 80cm in length (65cm to the detection window), with an applied voltage of 30kV.

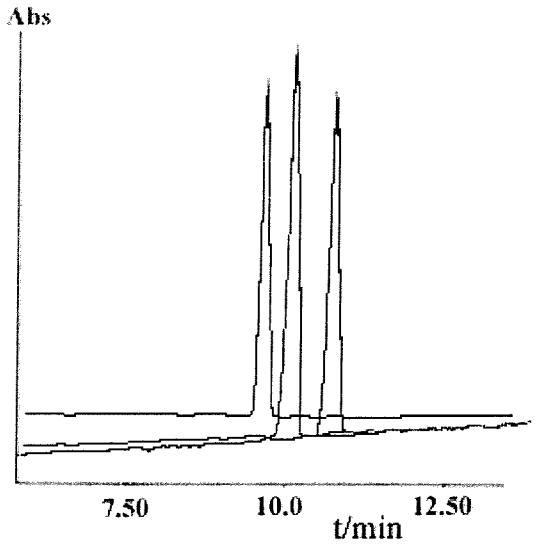

Fig. 3.6 Electropherograms of EDTA chelates of Ca, Mn and Cu. Peaks elute in the order CaEDTA, MnEDTA and CuEDTA.

As can be seen from Fig. 3.6 the peaks for Ca and MnEDTA would only just be resolved. Increasing the buffer concentration can help to increase the resolution of a separation at the expense of increased joule heating (more buffer ions $\Rightarrow$ higher current) and longer run time. Joule heating can cause loss of resolution due to peak broadening and also increased background noise. Many commercially available CE instruments have the capability of maintaining the column at a constant temperature to help negate the problems associated with joule heating.

A new buffer was prepared containing 100mM boric acid (adjusted to pH 9.5) and the samples were reanalysed using the conditions described previously. The resolution between Ca and MnEDTA increased slightly as did the baseline noise (due to increased joule heating); the current drawn by the system had increased from ~ 80μA to ~ 120μA.

Another way of increasing resolution is to use an organic modifier. An additional advantage of using an organic modifier is that it can reduce the current drawn by the system and hence reduce any effects due to joule heating.

Further buffers were prepared containing 100mM boric acid and varying amounts of methanol (from 5 to 10%v/v) and the samples re-run. From the results obtained, it was decided to use a methanol concentration of 6%, as this gave a more than adequate separation without an excessively long run time. Methanol was chosen as the organic modifier to avoid any possible problems with precipitation/solubility of the buffer salts, which can happen with acetonitrile at high pH.

Using this buffer system, samples of Pseudocatalase cream were prepared and analysed (see Fig 3.7). Two peaks seen in all samples and placebos analysed have been identified (using known standards) as 4-hydroxypropylbenzoate and 4-hydroxymethylbenzoate with migration times of about 8 and 9 minutes respectively. These compounds are commonly used as preservatives in the cosmetic and pharmaceutical industry.

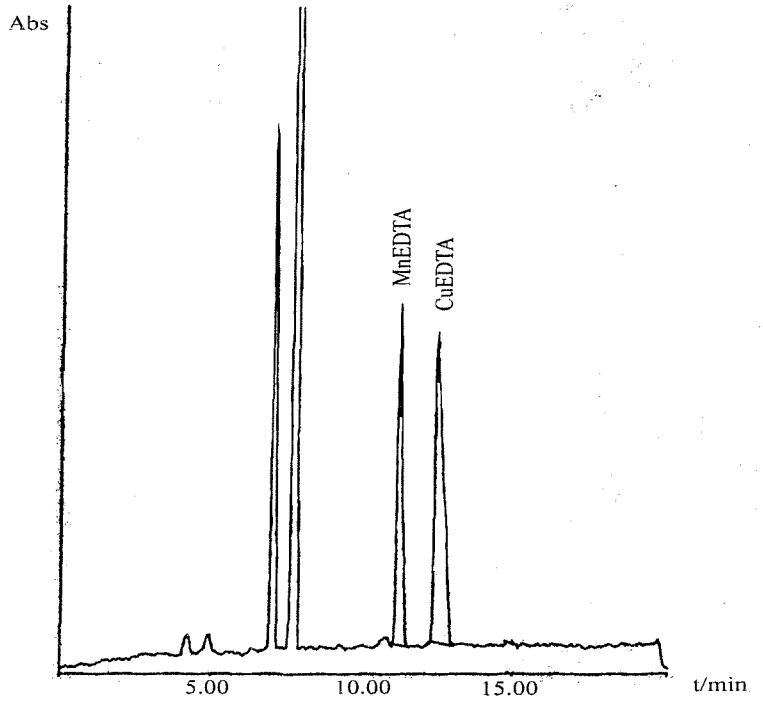

Fig. 3.7. Electropherogram of Pseudocatalase cream sample, using conditions described above.

It should be noted that in Fig. 3.7 no calcium EDTA is seen, even though calcium is present in the formulation, this is because of the difference in stability constants between the EDTA chelates of Mn and Ca (10.96 and 14.04 respectively) [32,33]. EDTA will form a stronger more stable complex with Mn than with Ca.

The method was subsequently validated in accordance with the current International Committee for Harmonisation (ICH) guidelines for the validation of analytical methods [34].

During the validation process it became apparent that a peak, (identified as 4-hydroxybenzoic acid a degradation product of the 4-hydroxybenzoates via hydrolysis) visible in aged samples, was drifting (reducing migration time) during the analysis of samples and almost co-migrating with the CuEDTA (internal standard) peak. The migration time for this peak gradually reduces from greater than 20 minutes to about 13 minutes over a period of 40 to 50 sample injections. A probable explanation for this is the column was contaminated by either the surfactants or any free metal ions present in the formulated product. It should be noted that the drift in migration time did not appear to effect the Mn, Ca or Cu EDTA chelates. This problem was remedied by flushing the column with 0.5M HCl in 50% methanol/water for 20-30 minutes after every 5-6 sample injections followed by reconditioning of the column with NaOH and buffer solution. The HCl was used to protonate the silanol groups on the capillary wall and to strip out any adsorbed/precipitated metals. Whilst the methanol was used to dissolve any surfactant adhering to the capillary wall.

Although this was successful, it was not practical for the routine analysis of batches containing upwards of 40 samples (especially if samples were being run overnight). Rather than change the analytical conditions to overcome this problem it seemed easier to find an alternative internal standard.

Other possible internal standards investigated were salicylic acid, potassium sorbate and 4-aminobenzoic acid; these were chosen because of their availability, good absorbance at low wavelength and they are ionised at the pH of the buffer. Both salicylic acid and potassium sorbate comigrated with possible degradation peaks or calcium EDTA. Of the three possible internal standards, 4-aminobenzoic acid appeared to be the best, (being well resolved from any other peaks). Therefore, the previous method was revalidated using this as the internal standard with the finalised details and procedures as follows.

Electrophoretic Conditions

Column:	Unmodified fused silica, 80cm length (65 cm effective)*, 50μm internal diameter.
Temp:	35°C
Detection:	Direct UV at 195 nm
Buffer:	100mM Boric Acid 60 mM NaOH 6% Methanol pH 9.5
Voltage:	30kV (electric field 375 Vcm^{-1})
Injection Mode:	+ve pressure 50 mbar for 18 seconds
Water:	18 MΩ water (BS3978 Grade 1) was used at all times.

* The effective length of the capillary is defined as the length from the injection end to the position of the detection window.

Buffer Preparation

6.183g of boric acid (99%+) and about 2.40g of NaOH were accurately weighed into a 1000ml volumetric flask. 60ml of methanol and about 900ml of water were added and the solution was shaken to dissolve. The pH of the buffer was adjusted to 9.50 - 9.60 with 1.0M NaOH, and made up to volume with water. The buffer was filtered through a 0.45μm Nylon filter before use.

Internal Standard Solution

About 0.50g of 4-aminobenzoic acid was accurately weighed into a 500ml volumetric flask and made to volume with methanol.

Standard Preparation (Prepared in duplicate)

About 0.50g of disodium manganese EDTA was accurately weighed into a 100ml volumetric flask and diluted to volume with water. 10.0ml of this solution was transferred by pipette into a clean 100ml volumetric flask. To this was added 10.0ml of 2.3% aqueous sodium bicarbonate solution, 20ml of methanol and 5.0ml of the internal standard solution, and made up to volume with water. The solution was filtered through a 0.45μm Nylon filter (to remove any particulate matter, which may block the capillary) into an autosampler vial for analysis.

Sample Preparation

About 10.0g of the sample (or placebo) was accurately weighed into a 100ml volumetric flask and 20ml methanol added. 5.0ml of the internal standard solution and about 40ml of water were added and then placed in an ultrasonic bath for 10 minutes to disperse the sample. The solution was made up to volume with water and mixed well. The solution was filtered through a 0.45μm Nylon filter into an autosampler vial for analysis.

Analysis

The capillary column was conditioned by flushing with 0.5M NaOH for 20-30 min followed by water for 10 min. Buffer was prepared as outlined previously and the column flushed with buffer for at least 30 min. Two vials of buffer were placed in the CE autosampler and the injection programme was set as follows: -

Step 1 Buffer vial 1 2000 mbar for 2 min

Step 2	Buffer vial 2	2000 mbar for 0.5 min
Step 3	Sample	50 mbar for 0.3 min
Step 4	Buffer vial 2	+ 30 kV for 20 min

Buffer vial 1 is used to flush the capillary column and vial 2 is used as the running electrolyte.

A standard was injected three times to demonstrate reproducibility (less than 2% deviation of migration time and response). If the migration times were drifting then the standards were injected another three times. If this still failed to give reproducible migration times then the column was reconditioned as described above, and the standard injections repeated until a deviation of less than 2% was achieved.

After each batch of analysis the column was cleaned by flushing with 0.5M HCI in 50% methanol for 30 min followed by water for 10 min. The capillary was then reconditioned with 0.5M NaOH as described previously.

Relative Migration Times

4-aminobenzoic acid	1.00
Na_2 MnEDTA	1.28

Identification

Under the conditions described above, the presence/absence of Na_2MnEDTA is confirmed by comparison of sample and standard electropherograms. The presence of a peak in the sample electropherogram with a migration time corresponding to a peak in the standard electropherogram is taken to be indicative of the presence of Na_2MnEDTA in the product.

Typical electropherograms obtained from standard and sample solutions are shown in Figs. 3.8a and 3.8b, these show the peaks obtained for the internal standard, MnEDTA, and the preservatives 4-hydroxypropylbenzoate and 4-hydroxymethylbenzoate.

Fig 3.8a Standard electropherogram.

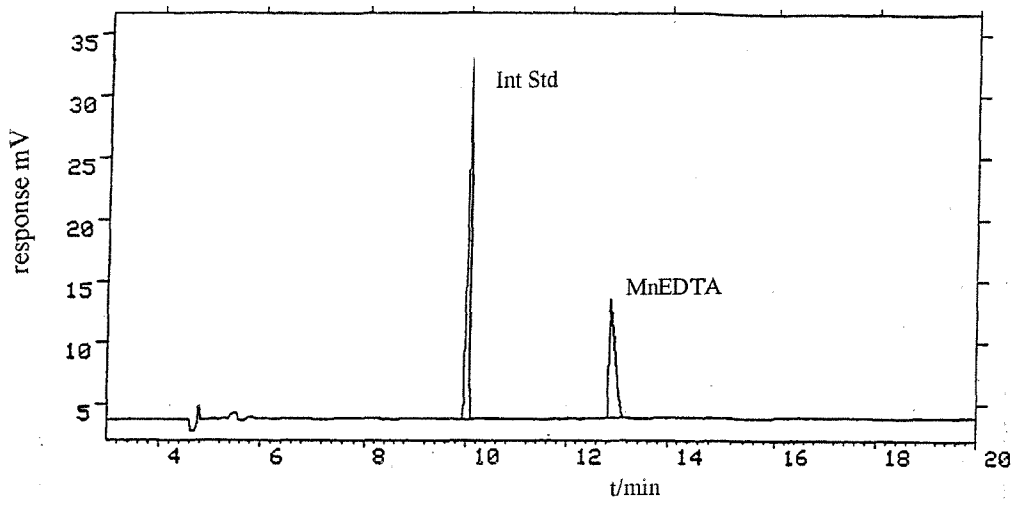

Fig. 3.8b Sample electropherogram.

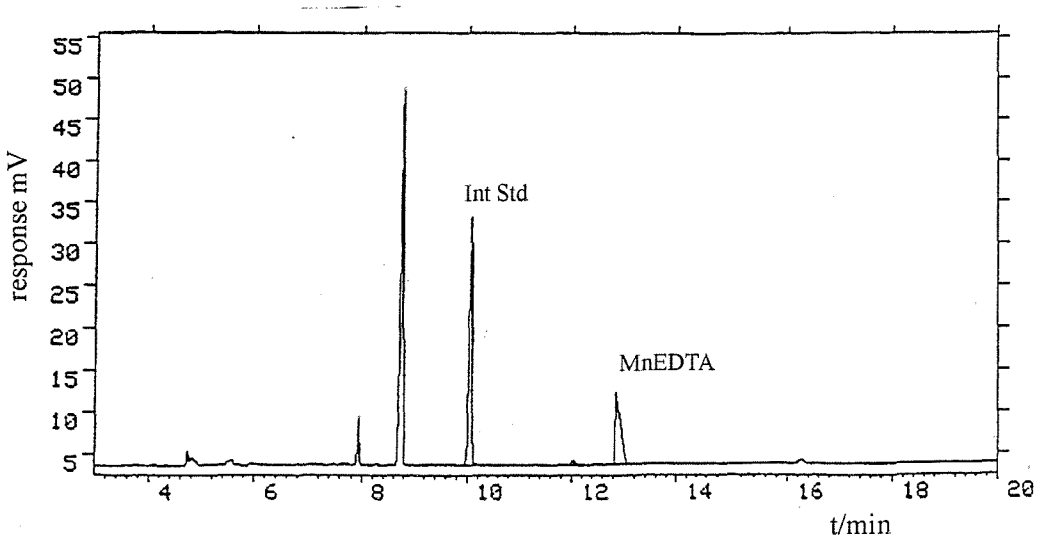

3.3 Validation of the method for the determination of disodium manganese EDTA in Pseudocatalase

The following standards were supplied by Aldrich Chemical Company (UK), and used throughout the validation.

disodium manganese EDTA	Lot number:	60716041 purity 88.8%
4-aminobenzoic acid	Lot number:	09111-076 purity 99.6%

Accuracy

The accuracy of the method was determined by performing a series of experiments at 50, 100 and 150% of the nominal concentration. The samples were prepared by adding known amounts of disodium manganese EDTA to the samples of Pseudocatalase placebo. Six samples were prepared at each level to be investigated. The accuracy was determined by calculating the percent recovery.

$$\% \text{ Recovery} = \frac{\text{Amount of analyte found}}{\text{Amount of analyte added}} \times 100$$

Table 3.1 $Na_2MnEDTA$: Accuracy at 50, 100 and 150% nominal concentration

	% Recovery		
Sample Number	50% nominal	100% nominal	150% nominal
1	97.5	100.1	98.2
2	98.1	99.5	100.7
3	98.2	99.9	100.2
4	97.9	99.9	99.6
5	98.6	99.3	100.6
6	98.3	100.8	100.7
Mean	98.1	99.9	100.0
%rsd	0.4	0.5	1.0

As the results for the recovery are between 98 and 102% with rsds less than 2% this indicates that the method is sufficiently accurate for its intended use

Precision

Repeatability

The precision of this method was determined by the analysis of six samples of Pseudocatalase (SF182/04/A). The data obtained for the analyses gave a mean of 0.47% w/w (0.9% rsd) for MnEDTA.

Reproducibility

To establish the reproducibility of this method a second operator analysed the same samples tested above (on a different day and a different instrument). This analysis gave a mean of 0.46% w/w with a rsd of 0.9%, compared with the mean value of 0.47% w/w determined by the first operator.

The results for both operators/instruments are given in table 3.2.

Table 3.2. First and second operator results for Pseudocatalase (SF182/04/A) %w/w MnEDTA

	1st Operator	2nd Operator
Sample	Instrument Serial No. 50-06-05-2-36	Instrument Serial No. 50-06-05-2-34
1	0.47 %w/w	0.47 %w/w
2	0.48 %w/w	0.46 %w/w
3	0.47 %w/w	0.46 %w/w
4	0.47 %w/w	0.46 %w/w
5	0.47 %w/w	0.46 %w/w
6	0.47 %w/w	0.46 %w/w
Mean	0.47 %w/w	0.46 %w/w
%rsd	0.87	0.88

These results demonstrate that the method is reproducible.

Linearity

The linearity of the response to the analyte was determined both in the presence and in absence of placebo, over the range of 0 - 200% of nominal concentration. The samples were prepared by dilution of a stock solution of analyte to give the required concentration level (samples were injected in duplicate at each level tested). Regression analysis of the data obtained gave the following results.

Fig. 3.9 Linearity - Absence of placebo.

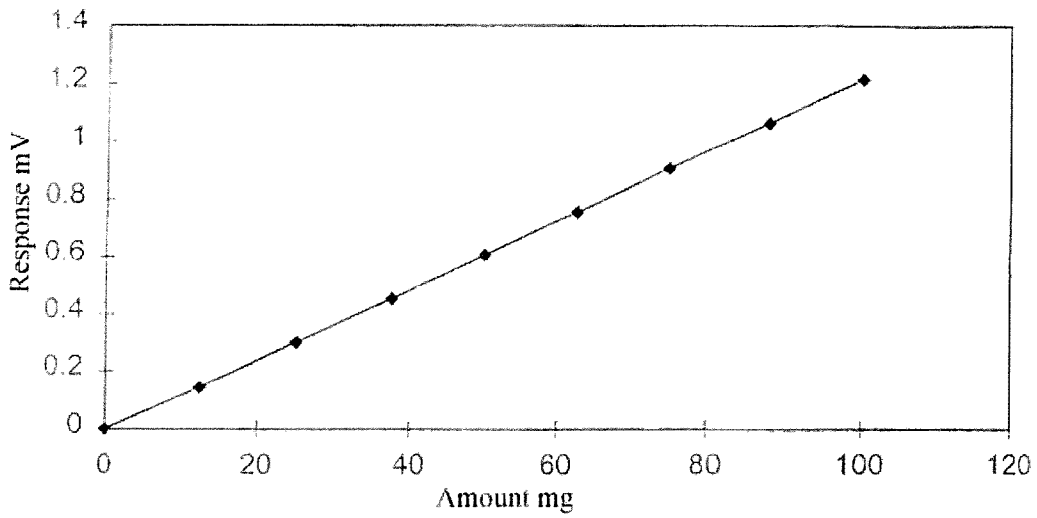

Intercept	-0.0057 mV
Slope	12.2 mV/mg
Regression coefficient, r	0.9997
p	<0.001

Fig. 3.10 Linearity - Presence of placebo.

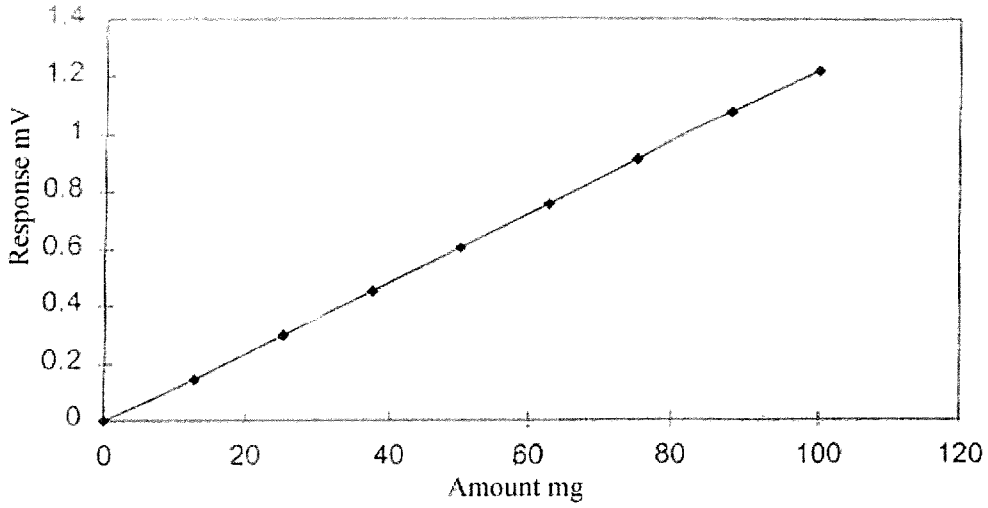

Intercept	-0.0081 mV
Slope	12.3 mV/mg
Regression coefficient, r	0.9998
p	<0.001

These data indicate that the response of $Na_2MnEDTA$ is linear with respect to the concentration over the range examined. Comparison of the slopes and intercepts indicates that there is no interference from the sample matrix. This justifies the use of single point calibration in the analysis of $Na_2MnEDTA$ in Pseudocatalase.

Specificity

Solutions of Pseudocatalase and Pseudocatalase Placebo (without disodium manganese EDTA) were subjected to conditions likely to cause degradation. Analysis of these solutions should show whether any peaks from the degradation of the analyte or matrix will interfere with the peaks of interest.

Conditions used: -

Heat: 10.0g of sample in 5.0ml of water, heated at 70°C for 17 h, in the dark.

Light: 10.0g of sample in 5.0ml of water, exposed to simulated sunlight (92,000 Lux) for 16 h (approx. equivalent to 10 days natural sunlight)

Acid: 10.0g of sample in 5.0ml of 0.5 M HCl, stored at room temperature, in the dark, for 168 h (7 days).

Base: 10.0g of sample in 5.0ml of 0.5 M NaOH, stored at room temperature, in the dark, for 168 h (7 days).

Oxidation: 10.0g of sample in 5.0ml of 3.0% H_2O_2, stored at room temperature, in the dark, for 168 h (7 days).

Control solutions of the samples and placebos were prepared. These were stored at room temperature, in the dark, for 168 h. (Control samples, wrapped in foil, were also placed in the light box). As heat is generated in the light box this will indicate if any degradation peaks are formed by the action of heat alone.

After the prescribed period, the samples were analysed; the internal standard was not added to these solutions to determine whether any peaks would interfere with it (see Figs. 3.11 to 3.24).

Results

Fig. 3.11 Control Sample

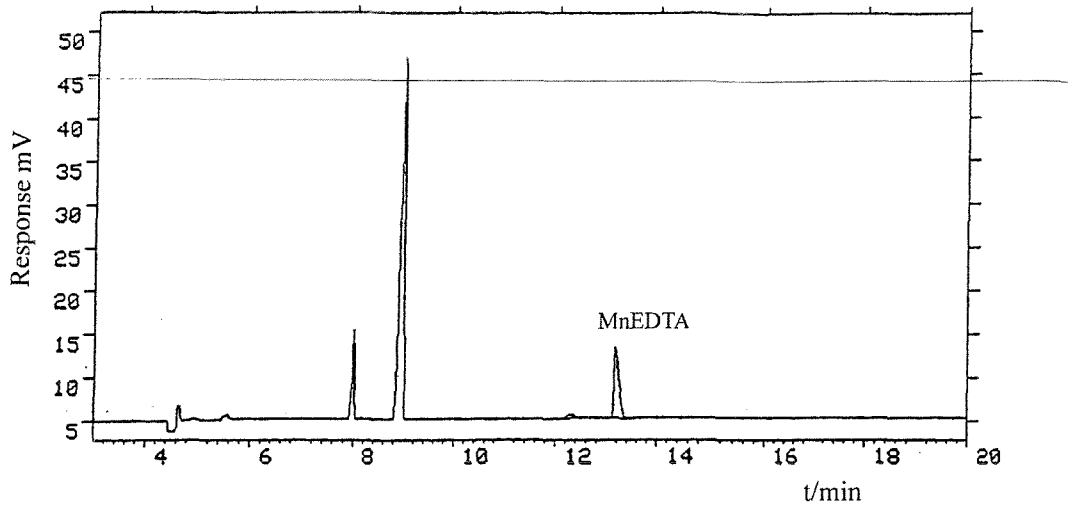

Fig. 3.12 Control Placebo

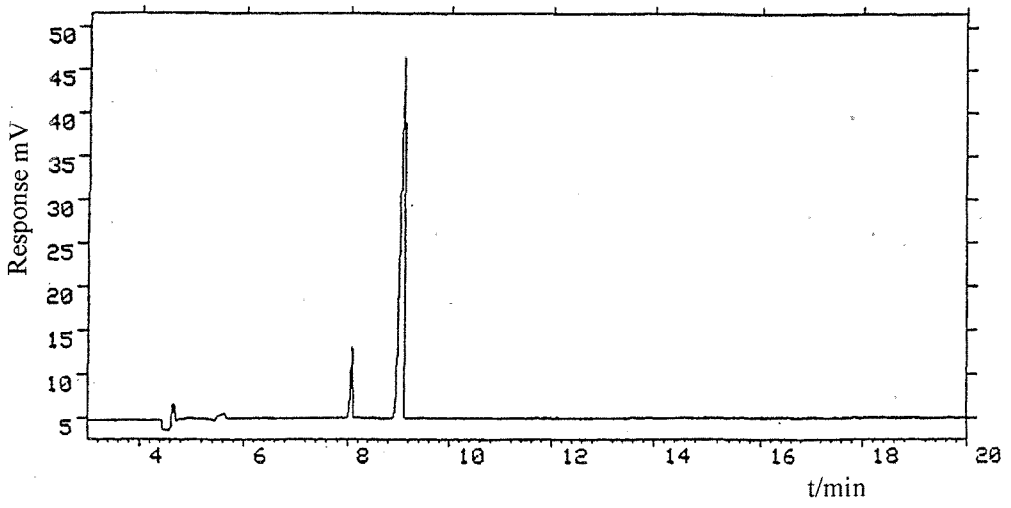

Control samples show no evidence of interference from the matrix with MnEDTA, internal standard or CaEDTA. The peaks seen at about 8 and 9 minutes are due to the preservatives 4-hydroxypropylbenzoate and 4-hydroxymethylbenzoate, respectively. A small peak seen in the sample at about 12 minutes is due to CaEDTA The baseline disturbance at 4.5 minutes is due to the EOF and the peak at 5.5 minutes is an unidentified excipient.

Fig. 3.13 Heated Sample

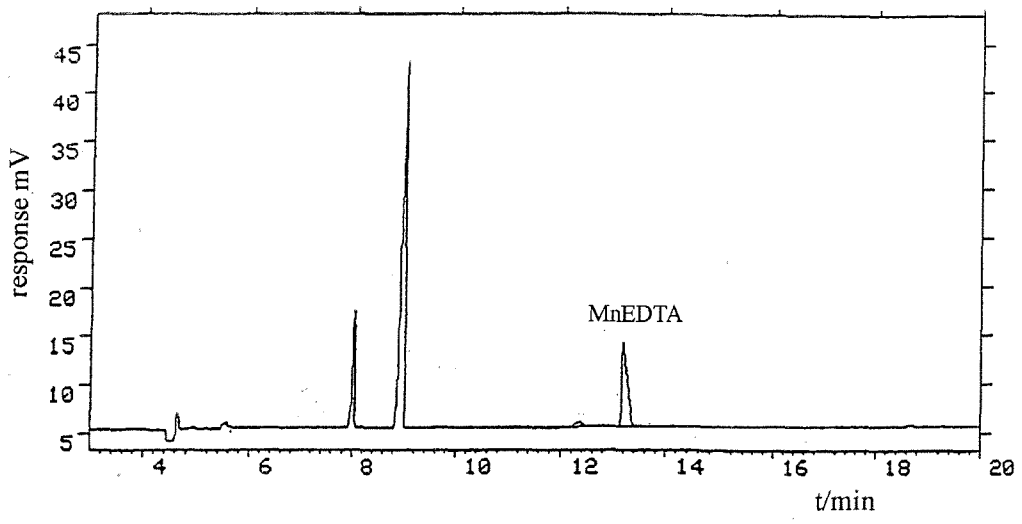

Fig. 3.14 Heated Placebo

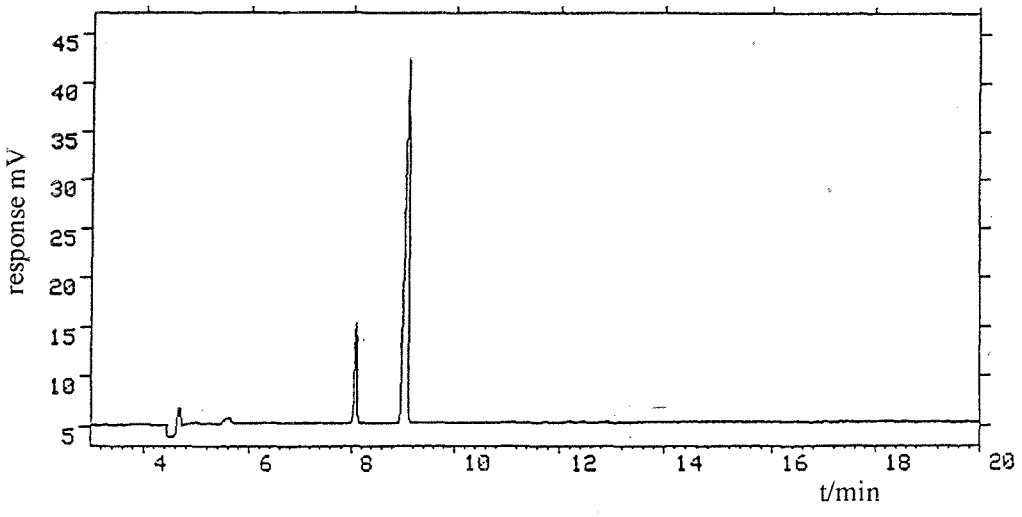

Heated samples show no evidence of degradation of MnEDTA or any interference from the matrix

Fig. 3.15 Acidified Sample

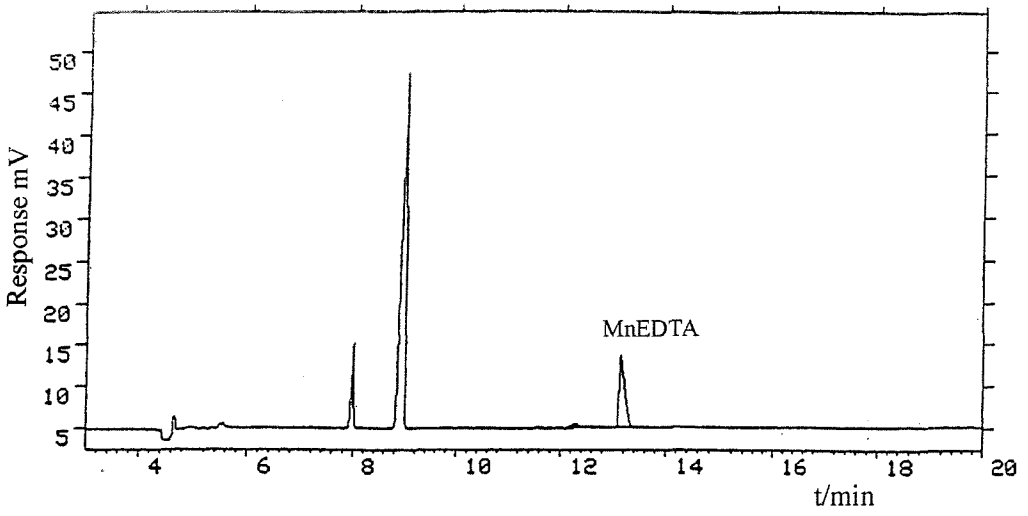

Fig. 3.16 Acidified Placebo

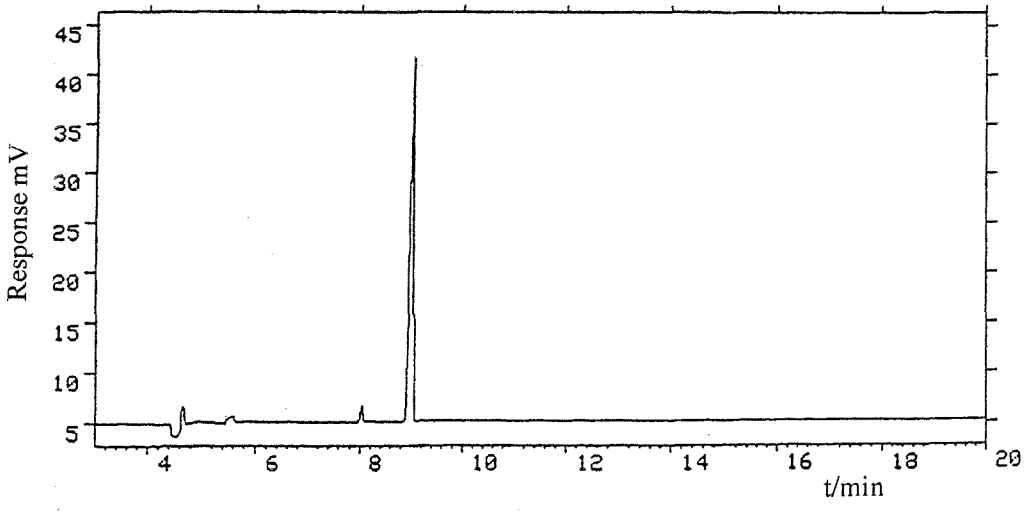

There is no evidence of MnEDTA degradation in acidified samples. Some reduction in the intensity of the methyl and propyl hydroxybenzote peaks, most probably due to acid hydrolysis was seen. No interference from the matrix was visible

Fig. 3.17 Sample in Base

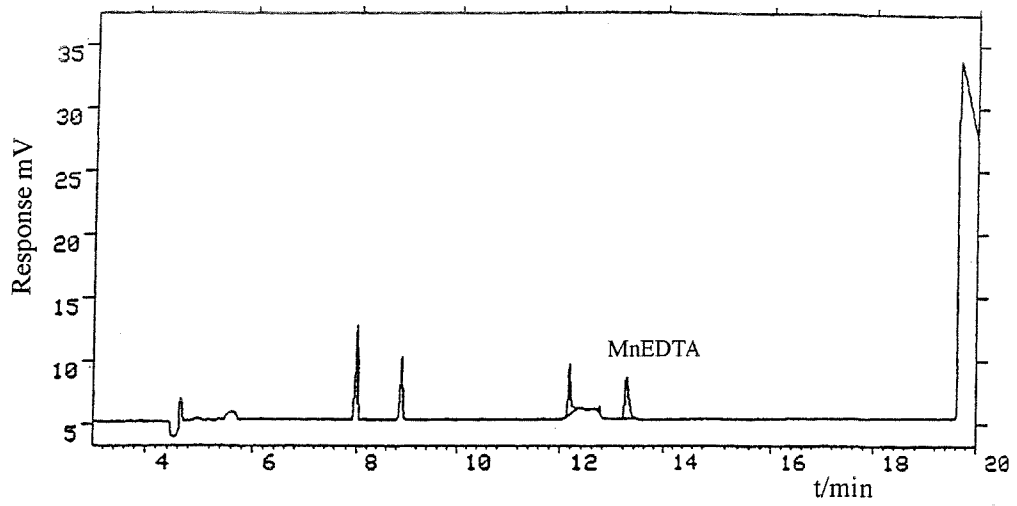

Fig. 3.18 Placebo in Base

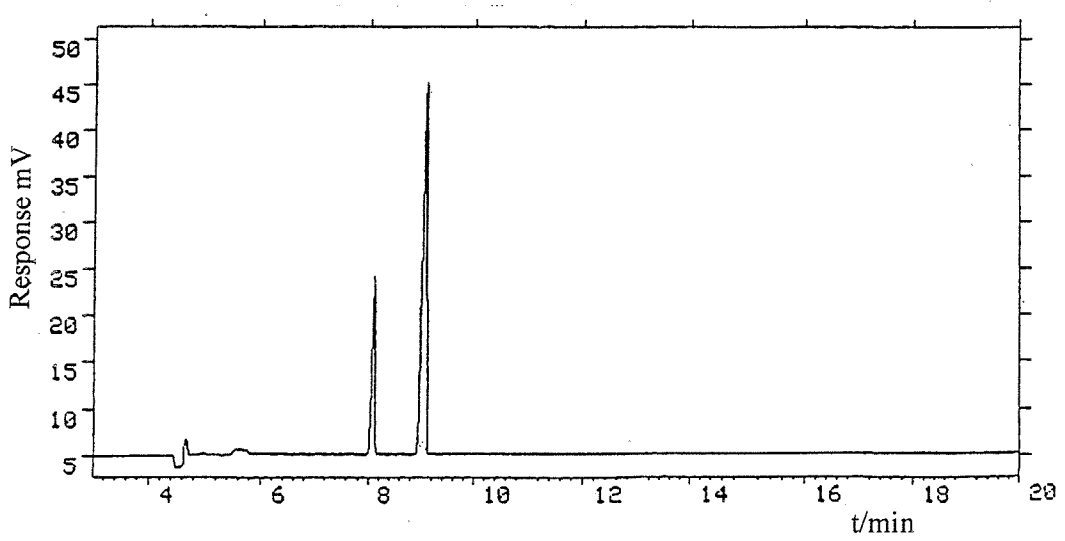

Extensive degradation of MnEDTA and the two preservatives can be seen in the sample exposed to NaOH. Peak seen at about 12.2 minutes is probably due to CaEDTA (the manganese has reacted with the base to form manganese hydroxide (dark precipitate seen in this sample) leaving the released EDTA to complex with Ca. The peak at 19.5 minutes is from the hydrolysis of the preservatives and has been identified as 4-hydroxybenzoic acid (by matching migration time of a known reference sample). It is not clear why degradation of the preservatives has not occurred in the placebo sample, (possible catalysis of the hydrolysis of the preservatives by the presence of the metal ions in the sample).

Fig. 3.19 Oxidised Sample

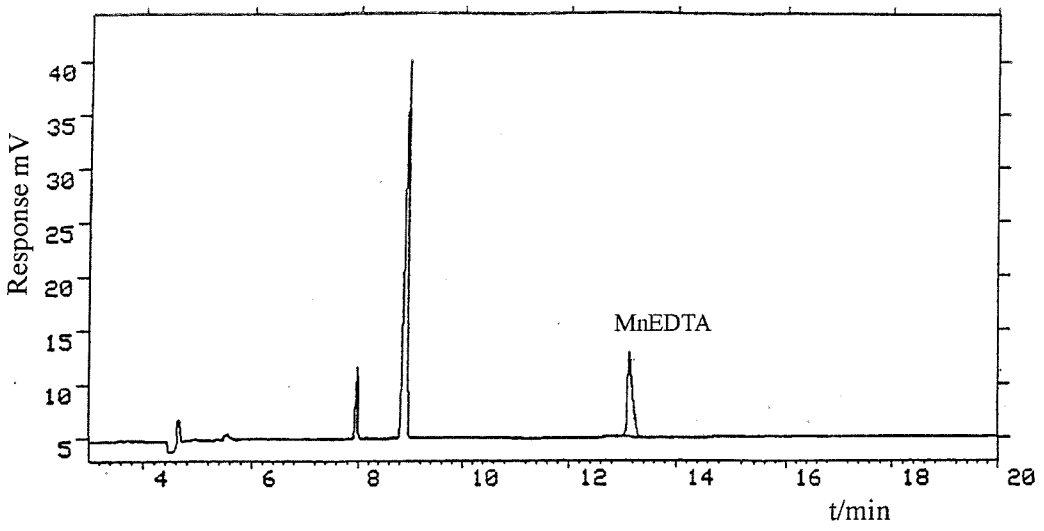

Fig. 3.20 Oxidised Placebo

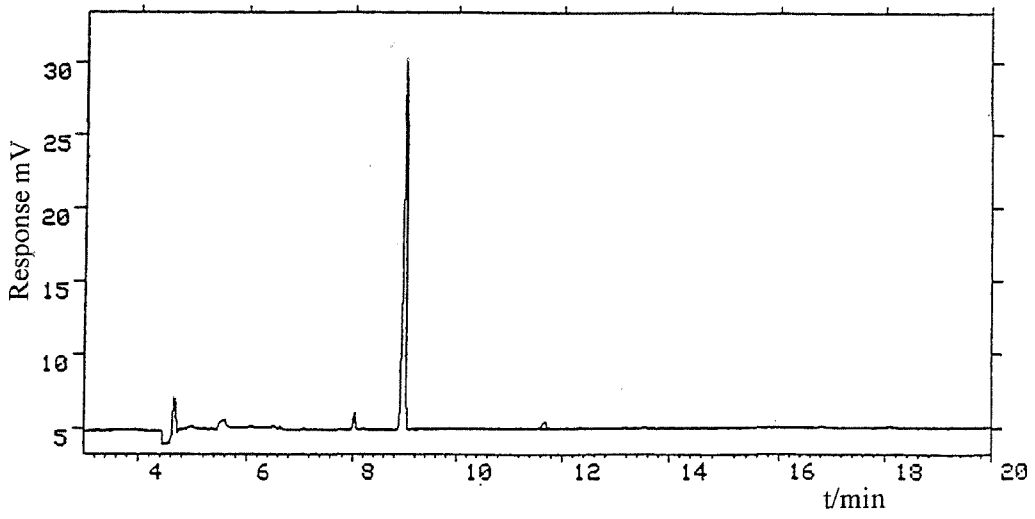

Oxidised samples show some evidence of degradation of the preservatives, this appears to be more pronounced in the placebo sample. This is probably due to the breakdown of H_2O_2 in the sample containing MnEDTA (H_2O_2 is known to rapidly degrade to water and oxygen in the presence of small amounts of metals), thus effectively reducing the concentration of H_2O_2 in this sample. A small peak seen at 11.5 minutes has not been identified but it is well resolved from the peaks of interest.

Fig. 3.21 Light Exposed Sample

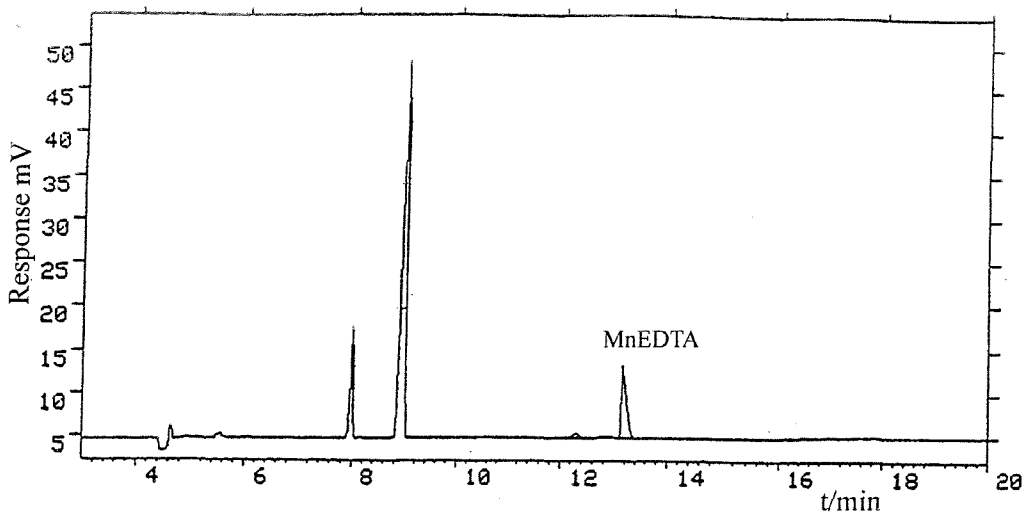

Fig. 3.22 Light Exposed Placebo

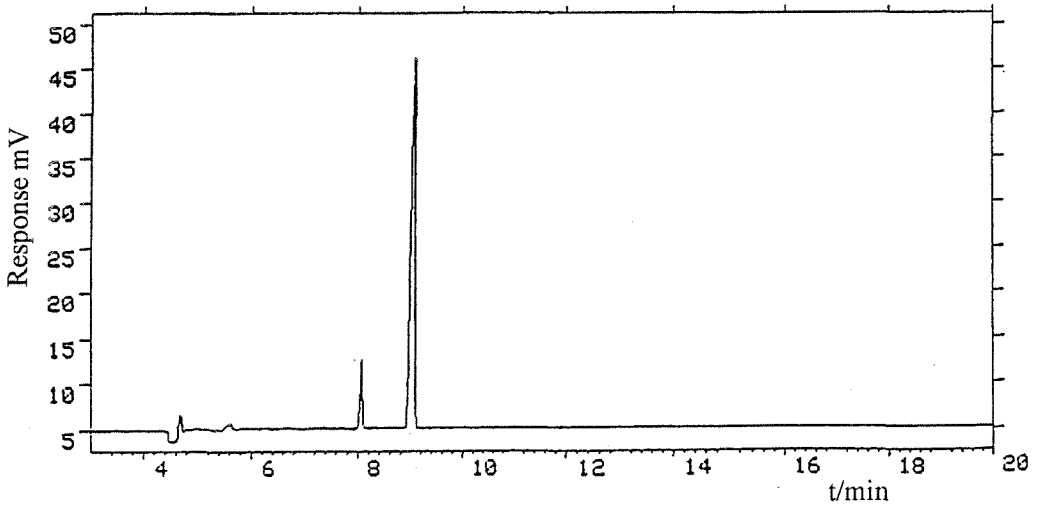

Fig 3.23 Light Exposed Sample Control

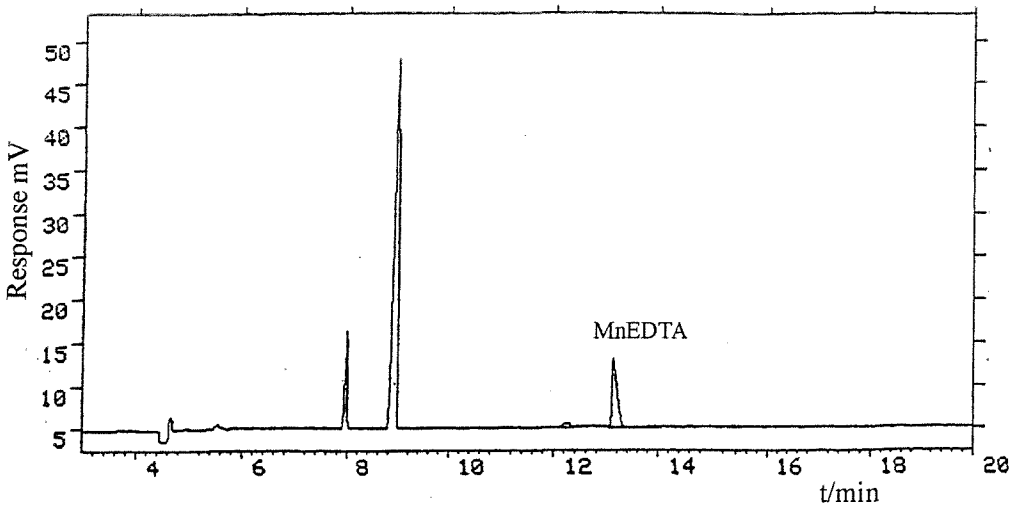

Fig. 3.24 Light Exposed Placebo Control

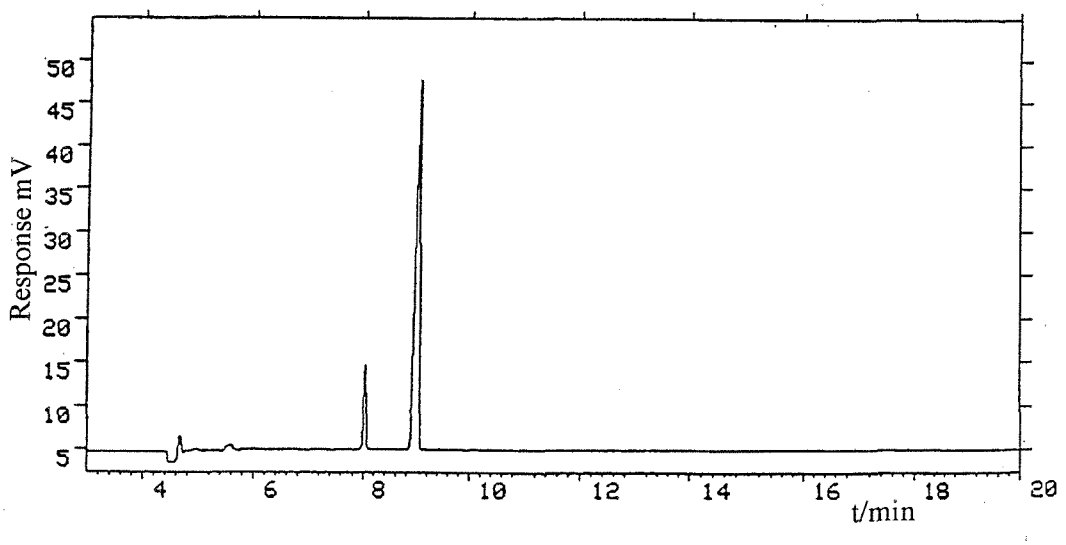

Light exposed samples and controls show no evidence of degradation of MnEDTA or any interference from the matrix

Ruggedness

Changing the apparatus, operator and date of assay (see precision results Table 3.2) gave an indication as to the ruggedness of this method. First analysis was performed on CE2 serial number: 50-06-05-2-36 (comprising a buffer control unit serial number: 55-05-01-0-12 and Unicam detector serial number: 408130). Second analysis was performed on CE3 serial number: 50-06-05-2-34 (comprising a buffer control unit serial number: 55-05-01-0-09 and Unicam detector serial number: 408131).

Deliberate changes to the buffer composition (wrt pH and organic modifier) were also made and examined, as these are the factors most likely to affect the separation.

These results are shown in table 3.3 where the assay result is the mean of six analyses.

Table 3.3 Results of changes made to the buffer solution.

	Assay % w/w		Relative mobility	Degradation
Change	mean	rsd	$Na_2MnEDTA$	peak
None	0.46	0.4	1.18	*
pH 9.0	0.45	0.3	1.19	about 15 min
pH 10.0	0.46	2.2	1.19	*
3% Methanol	0.44	0.4	1.19	18-19 min
9% Methanol	0.45	0.4	1.18	*

* Degradation peak not detected within the run time of 20 min.

The relative mobility was calculated to give a better indication to the changes occurring in the separation process (as it takes into account changes in the EOF due to pH, organic content etc). Itwas calculated as follows: -

$$\text{Relative mobility} = \frac{\text{mobility of analyte}}{\text{mobility of internal std}}$$

where mobility $= \frac{l \times L}{t_a \times v} - \frac{l \times L}{t_{eof} \times v}$

and

l = effective length of capillary L = total length of capillary

t_a = migration time of peak t_{eof} = migration time of neutral marker

v = applied voltage

As can be seen from the results in table 3.3 the changes made to the buffer composition appear to have no significant effect on the determination of the amount of MnEDTA in the samples.

3.4 Conclusion

This Chapter has shown that capillary electrophoresis can be used as a stability indicating method for the analysis of MnEDTA in Pseudocatalase. It can also be seen that with a small amount of data about the analyte (such as pK_a and solubility) methods can generally be developed within a matter of days, unlike HPLC where development of a method may take several weeks. We have also shown that a capillary electrophoresis method can be validated in a similar manner to HPLC methods.

Summary of Validation

The assay for disodium manganese EDTA is specific, precise, accurate, linear and rugged within the range and conditions studied. This indicates that the method is suitable for use as a stability indicating method.

Specificity	- Confirmed to be specific for the analyte except under conditions of extreme alkalinity.
Precision	- Confirmed by the relative standard deviations obtained from the replicate analysis (n=6) of a single sample performed by two different operators on different equipment. Rsd operator 1 = 0.9%. Rsd operator 2 = 0.9%

Accuracy	- Confirmed by the replicate (n=6) assay of three sets of placebo spiked at 50, 100, 150% of nominal concentration of analyte. The mean recoveries were 98.1%, 99.9%, 100.0%, with rsd's of 0.4%, 0.5%, 1.0% respectively.
Linearity	- Determined over the concentration range 0 to 200% of nominal, both in the presence and in the absence of placebo. Regression analysis gave the following correlation coefficients:

r	=	0.99971	Absence of placebo
r	=	0.99981	Presence of placebo

Ruggedness	- Confirmed with respect to time, operator and equipment. Also proved regarding changes in buffer composition.

References

1. W. Bucherberger, P. R. Haddad and P W Alexander, *J. Chromatogr.*, **558,** 181, 1991.
2. M. Unger, E. Mainka and W. König, *Z. Anal. Chem.*, **329,** 50, 1987.
3. W. F. Lein and B. K. Boerner, *J. Liq.Chromatogr.*, **10,** 3213, 1987.
4. D. L. Venezky and W. E. Rudzinski, *Anal. Chem.*, **56,** 315, 1984.
5. D. G. Parkes, M. G. Caruso and J. E. Spradling III, *Anal. Chem.*, **53,** 2154, 1981.
6. J. H. Knox and M. Shibukawa, *J. Chromatogr.*, **545,** 123, 1991.
7. E. L. Inman, R. L. Clemens and B. A. Olsen, *J. Pharm. Biomed. Anal.*, **8,** 513, 1990.
8. L. Hall and L. Takahashi, *J. Pharm.Sci.*, **77,** 247, 1988.
9. A. Yamaguchi, A. R. Rajput, K. Ohzeki and T. Kambara, *Bull. Chem. Soc. Jpn.*, **56,** 2621, 1983.
10. A. Yamaguchi, A. Toda, K. Ohzeki and T. Kambara, *Bull. Chem. Soc. Jpn.*, **56,** 2949, 1983.
11. J. Harmsen and A. van der Toorn, *J. Chromatogr.*, **249,** 379, 1982.
12. J. Dai and G. R. Helz, *Anal. Chem.*, **60,** 301, 1988.
13. G. A. Perfetti and C. R. Warner, *J. Assoc. Off. Anal.Chem.*, **62,** 1092, 1979.
14. H-J. Götze and D. Bialkowski, *Z. Anal. Chem.*, **323,** 350, 1986.
15. T. I. Lin, Y. H. Lee and Y. C. Chen, *J. Chromatogr.*, **654,** 167, 1993.
16. T. I. Lin and Y. H. Lee, *J. Chromatogr.*, **675,** 227, 1994.
17. A. R. Timerbaev, W. Buchberger, O. P. Semenova and G. K. Bonn, *J. Chromatogr.*, **630,** 379, 1993.
18. Q. Yang, C. Hartmann, J. Smeyers-Verbeke and D. L. Massart, *J. Chromatogr.*, **717,** 415, 1995.
19. T. Saltoh, C. Kiyohara and N. Suzuki, *J. High. Res. Chromatogr.*, **14,** 245, 1991.
20. T. Hirokawa, T. Ohta, K. Nakamura, K. Nishimoto and F. Nishiyama, *J. Chromatogr.*, **709,** 171, 1995.
21. I. Haumann and K. Bächmann, *J. Chromatogr.*, **717,** 385, 1995.
22. S. Hjerten, *Chromatogr. Rev.*, **9**, 122, 1967.
23. S.W.Compton and R.G.Brownlee, *Biotechniques,* **6**, 432, 1988.
24. O.Vesterberg, *J.Chromatogr.*, **480**, 3, 1989.
25. K. Kleparnik and P. Bocek, *J. Chromatogr.*, **569,** 3, 1991.

26. G. M. McLaughlin, J. A. Nolan, J. L. Lindahl, R. H. Palmieri, K. W. Anderson, S. C. Morris, J. A. Morrison, and T. J. Bronzert, *J. Liq.Chromatogr.*, **15,** 961, 1992.
27. A. D. Tran, S. Park, P. J. Lisi, O. T. Huynh, R. R. Ryall, and P. A. Lane, *J. Chromatogr.*, **542,** 459, 1991.
28. S. Terabe, K. Otsuka, K. Ichikawa, A. Tsuchiya and T. Ando, *Anal. Chem.*, **56,** 111, 1984.
29. J. E. Wiktorowicz and J. C. Colburn, *Electrophoresis,* **11,** 769, 1990.
30. R. L. Cunico, V. Gruhn, L. Kresin, D. E. Nitecki, and J. E. Wiktorowicz, *J. Chromatogr.*, **559,** 467, 1991.
31. S. Motomizu, M. Oshima, S. Matsuda, Y. Obata and H. Tanaka, *Anal. Sci.*, **8,** 619, 1992.
32. R. M. C. Dawson, D. C. Elliott, W. H. Elliott and K. M. Jones, Data for Biochemical Research, 3rd ed., Clarendon Press, Oxford (1986).
33. C R C Handbook of Organic Analytical Reagents (K. L. Cheng, K. Ueno, T. Imamura, eds.), C R C Press, Boca Raton (1982).
34. Text on validation of analytical procedures: methodology. International Conference on Harmonisation of Technical Requirements for the Registration of Pharmaceuticals for Human Use (ICH), IFPMA Ed., (Geneva, Switzerland, 1996).

Chapter 4

Analysis of Manganese EDTA Bicarbonate Complex by ESR.

4.1 Introduction

The aim of this chapter is to evaluate the use of ESR, as an analytical technique, for the analysis of the active component of Pseudocatalase in the final cream samples.

The majority of manganese (II) complexes are high spin, in an octahedral field this configuration gives spin-forbidden as well as parity-forbidden electronic transitions, thus accounting for the extremely pale colour of these compounds. The high spin d^5 configuration of Mn (II) gives an essentially spin-only, temperature-independent magnetic moment of ~5.9BM. The paramagnetic properties of manganese (II) make it an ideal candidate for analysis by ESR.

Theory

Electron spin resonance (ESR) spectroscopy is a useful technique for studying atoms or molecules that contain one or more electrons with unpaired spins, since such types of compounds are also paramagnetic, this type of spectroscopy is often referred to as electron paramagnetic resonance (EPR) [1,2,3].

Substances with unpaired electrons can arise naturally (such as ions of transition metals) or artificially. The latter are unstable and are usually called free radicals or radical ions; they are often formed as intermediates in a chemical reaction. The magnetic moment of an unpaired electron is about 700 times that of the proton, so that the sensitivity of ESR detection is very much higher than in NMR. This is fortunate, since the concentrations of compounds with unpaired electrons are often correspondingly lower: ESR spectra can be recorded for radical concentrations down to 10^{-4}M, irrespective of the number of non-radical species present. Provided the lifetimes of the radicals are greater that about 10^{-6} s, they may be studied using ESR techniques. Short-lived species may be examined by producing or trapping the

radicals at low temperatures (e.g. by using liquid nitrogen) or by chemical reactions to form a stable product such as

$$R^{\bullet} + \text{nitrone} \rightarrow \text{Rnitroxide}$$

The compounds used for these types of reactions are often known as 'spin traps', for example, 5,5-dimethyl-1-pyrroline *N*-oxide (DHPO) is commonly used as a spin trapping reagent for the study of hydroxyl and superoxide radicals; its structure is

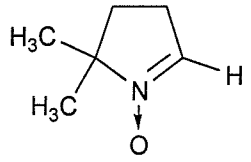

When unpaired electrons exist in a substance, their spins are aligned at random in the absence of any external influence. When placed in a magnetic field, however, they will each have a preferred direction and, since the spin of an electron is ½, each electron can be thought of as spinning either clockwise or anticlockwise about the field direction. ESR spectroscopy essentially measures the amount of energy needed to reverse the spin of an unpaired electron and it is the information contained in this energy that enables us to make deductions on the properties of the material being studied.

As in all forms of spectroscopy, four properties of the spectral lines are of importance – the intensity, width, position and multiplet structure. The intensity of the line is proportional to the concentration of the paramagnetic material present. Thus, in theory, we have a technique for estimating the amount of material present, albeit not very accurate in practice. The width of the resonance depends on the spin relaxation time of the system under study. Of the two possible relaxation processes, the spin-spin interaction is usually very efficient and gives a relaxation time of the order of 10^{-6} to 10^{-8} s. The spin-lattice relaxation is efficient at room temperature (typically 10^{-6} s) but becomes progressively less so at reduced temperature (several minutes at the temperature of liquid nitrogen). Using the Heisenberg uncertainty principle:

$$\delta\nu = \frac{\delta E}{h} \approx \frac{h}{2\pi h \delta t} \approx \frac{1}{2\pi\delta t} \qquad \text{Eq 1}$$

and a typical relaxation time (δt) of 10^{-7} s, will give a linewidth of about 1MHz. A shorter relaxation time will increase this width and 10MHz is not uncommon (typical linewidths for NMR are in the order of 0.1Hz). It should be noted that in ESR it is the field rather than the frequency that is used to scan the spectra.

The wider lines found in ESR have both advantages and disadvantages. The advantages are that the homogeneity of the applied magnetic field is far less critical, for ESR a field homogeneous to 1 in 10^5 is usually adequate (compared to 1 in 10^8 for NMR). One of the main disadvantages is that the broad lines produced in ESR spectra can mask any effects equivalent to the NMR chemical shift, as the effects influencing the g factor are much larger. The position of the absorption can be seen to vary directly with the klystron frequency and the g factor, thus for an electron in an applied magnetic field, B, the spin energy levels are separated by

$$\Delta E = g\mu_B B \qquad \text{Eq 2}$$

where μ_B is the Bohr magneton (9.273×10^{-24} JT^{-1}) and g is the Landé splitting factor. Since different ESR spectrometers operate at different frequencies, it is far more convenient to refer to the absorption in terms of its observed g factor. If we rearrange equation 2 then:

$$g = \frac{\Delta E}{\mu_B B} \qquad \text{Eq 3}$$

and if, for example, resonance was observed at 0.34 Tesla (T) in a field of 9.5 GHz, it would correspond to a sample with a g factor of 2.0023. This happens to be the g factor for a free electron; virtually all free radicals have a g factor that approximates very closely to this figure; and deviations from this value are caused by the coupling of the spin to the angular momentum of the electron in the molecular/atomic orbital containing it. In addition, the electron can be localised in a particular atomic orbital and the orbital angular momentum couples coherently with the spin angular momentum (spin-orbit coupling), giving rise to a g factor consistent with

$$g = \frac{3}{2} + \frac{S(S+1) - L(L+1)}{2J(J+1)} \qquad \text{Eq 4}$$

where S is the spin quantum number, L is the orbital momentum quantum number and J is the rotational quantum number (which, for condensed phases can be ignored). For example, the methyl radical has a g factor of 2.00255 and the benzene radical anion has a g factor of 2.00260. For these examples, all but one of the electrons in each molecule are paired so we only need to consider the spin motion of a single unpaired electron, hence, the g factors for these molecules nearly equals that of a free electron.

In ESR spectra there are two kinds of multiplet structure; there is the fine structure, which occurs only in species containing more than one unpaired electron spin, and the hyperfine structure (a smaller effect) which arises when an unpaired electron can get close to a nucleus with non-zero spin. In solution, the observation of hyperfine splitting indicates that the electron is in an orbital with s character. It is the interaction of the magnetic moment of the unpaired electron with those of any surrounding nuclei having a non-zero spin, which give rise to the hyperfine structure. The spin-orbit coupling is a significant contributor to the hyperfine interaction as it increases the "effective" total electron spin. This coupling is analogous to the coupling between nuclear spins seen in NMR spectra. As in NMR if more than one nucleus can interact with a given electron then the results can be predicted using Pascal's triangle.

Electron-nucleus coupling constants are much larger than those found for nucleus-nucleus interactions. This is dependant on the nature of the atomic orbital and the magnetogyric ratio ($\gamma_e = 1.77 \times 10^7\ s^{-1}\ G^{-1}$). For most organic molecules with an unpaired electron the coupling constants are of the order 10^{-4} to 10^{-3} T (2 to 20 MHz), and in ESR they are usually measured in T or Gauss, compared to the largest dipolar nucleus-nucleus coupling of about 2 kHz (10^{-7} T). Using the above examples of the methyl radical and benzene anion radical, the coupling constants are 2.3 and 0.38 mT respectively.

ESR spectroscopy is carried out in the microwave region, and many commercially available instruments use a klystron source at a fixed frequency of about 9.5 GHz with an electromagnet producing a field of about 0.34 T so it can easily be swept through and the spectra recorded. (These values are used to produce a resonance for a g factor = 2).

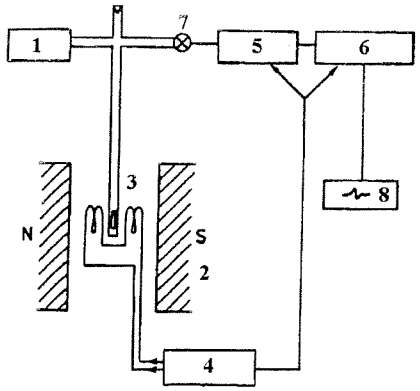

Fig. 4.1 Block diagram of ESR spectrometer, 1 klystron, 2 electromagnet, 3 sample in cavity resonator, 4 field modulator, 5 amplifier, 6 rectifier, 7 crystal detector, 8 output.

Additional Helmholtz coils are fitted to supply an oscillating magnetic field of a few microtesla and at a frequency of several hundred kHz. This provides a modulator (or chopper) frequency to which the detector system may be tuned in order to improve the signal to noise ratio; this means that the spectrum appears in the derivative mode. In regions where the absorption spectrum varies slowly the signal change monitored over each cycle of the modulation is small, whereas when the spectrum changes rapidly with the field, the signal change is large (see Fig. 4.2).

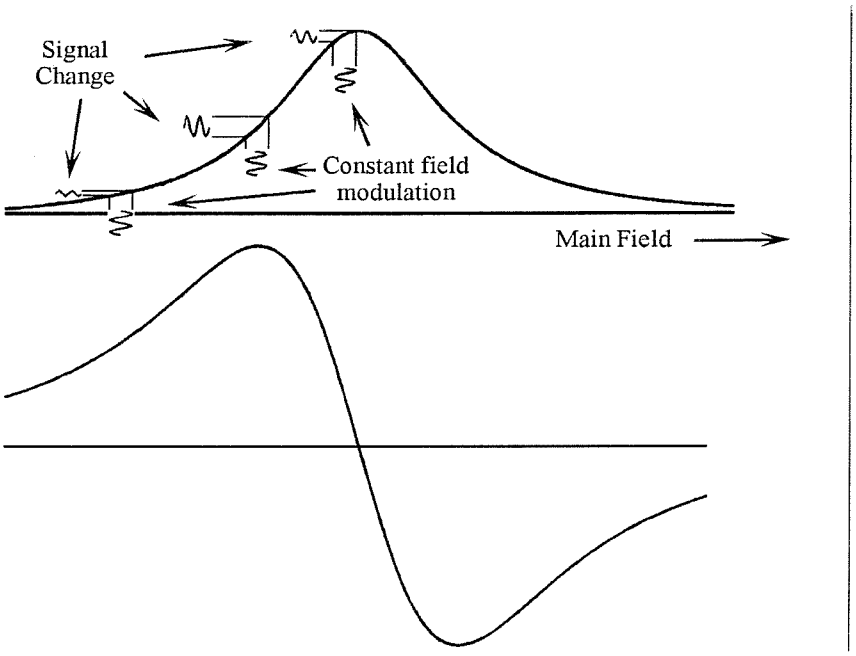

Fig 4.2. An absorption spectrum showing the constant amplitude of the field modulation and consequent signal change leading to the corresponding first derivative spectrum.

Thus the signal change measures the slope of the spectrum and this can then be recorded directly as the first derivative curve. This has two advantages: the point of maximum absorption is easier to measure accurately and it is easier to estimate the peak-width of a derivative signal than that of a corresponding broad absorption spectrum.

As transition metals have a significant orbital angular momentum, the spin-orbit coupling will also be quite large, and any metal ion with an odd number of unpaired electrons should give a well-defined ESR signal.

Manganese chloride in solution (the stating point for the formation of Pseudocatalase) exists as the 2+ ion with six water molecules co-ordinated (on average) in an octahedral configuration (see Fig. 4.3). Because of the symmetry of this complex we would expect to see six equally spaced hyperfine lines of equal intensity (see Fig 4.4) due to the interaction of the five unpaired electrons in the *d* orbitals, with the nuclear spin of manganese (which is 5/2).

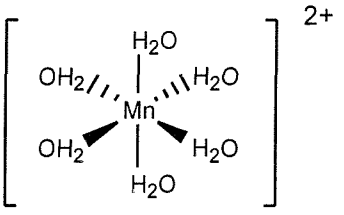

Fig 4.3 $[Mn(H_2O)_6]^{2+}$ in solution

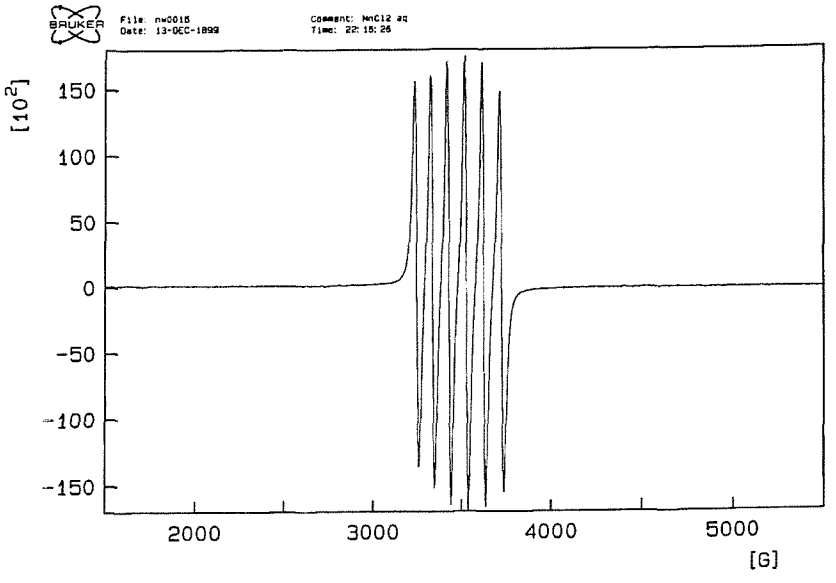

Fig. 4.4 Typical ESR spectrum of manganese chloride in solution

4.2 Experimental

As these samples are mainly aqueous based a flat quartz cell was used instead of the standard ESR sample tubes. The reason for this is that the microwaves produced in the sample cavity will be absorbed by the water molecules and this produces a heating effect, which makes it impossible to tune the microwave cavity. The flat cell can be rotated within the sample cavity to present a minimal cross-sectional area with respect to the E vector of the microwave radiation and thus reduce this effect.

Stock solutions of manganese chloride, disodium EDTA, and sodium bicarbonate were prepared as follows:

1. Manganese chloride – $MnCl_2.4H_2O$ 0.375% w/w in water (= 0.2mM)
2. Disodium EDTA – $Na_2EDTA.2H_2O$ 0.707% w/w in water (= 0.2mM)
3. Sodium bicarbonate – $NaHCO_3$ 2.30% w/w in water (= 2.74mM)

The stock solutions were then diluted as follows to give the final test solutions (with a concentration equivalent to a 1 in 10 dilution of Pseudocatalase cream):

a. 10.0ml of solution 1 in 100ml water
b. 10.0ml of solution 2 in 100ml water
c. 10.0ml of solution 3 in 100ml water
d. 10.0ml of solution 1 and 10.0ml of solution 3 in 100ml water
e. 10.0ml of solution 1 and 10.0ml of solution 2 in 100ml water
f. 10.0ml each of solutions 1, 2 and 3 in 100ml water

The solutions were placed in the flat cell and the spectra recorded. The cell was washed with deionised water, dilute HCl and dried with acetone between each analysis. A spectrum of water was also recorded as a reagent blank.

The following instrument parameters were used:
Receiver Gain = 4.00×10^5, mod frequency = 100kHz, mod amp =3.197G
Field Centre = 3482.6G, sweep = 4000G, resolution = 1024 points
Signal conversion = 40.96ms, time const = 40.96ms, sweep time = 41.943s
Microwave power 12.6mW, frequency 9.468 GHz

Solutions b, c and the water blank showed no evidence of any ESR peaks (spectra not shown). Indicating that there is no significant background signal from the cavity and the absence of any paramagnetic impurities.

Spectra of solutions a, d, e and f are shown in figs 4.5 to 4.8

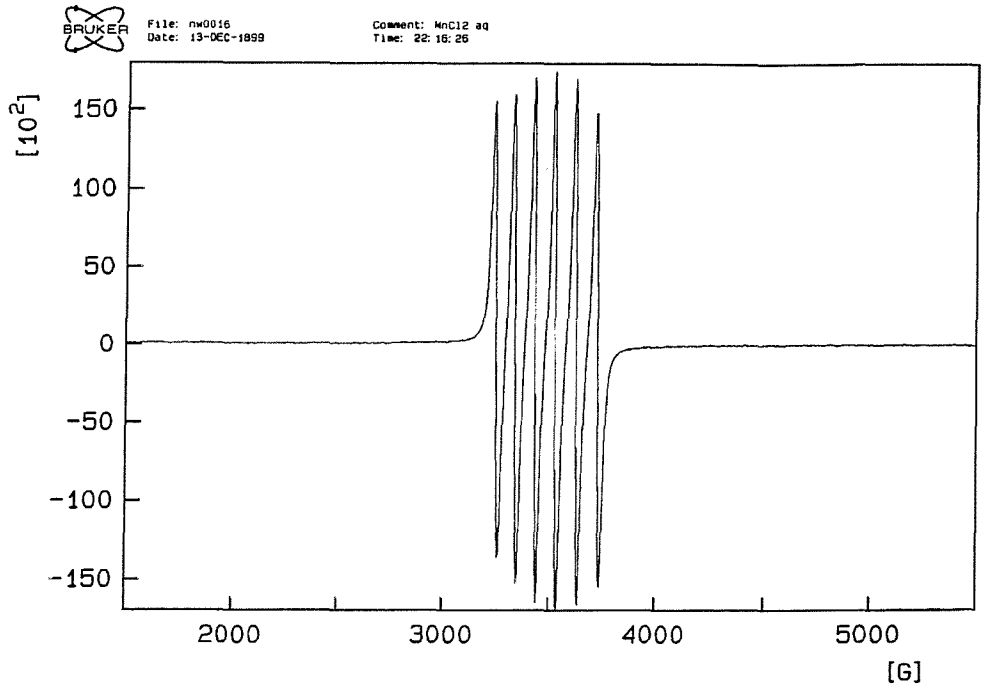

Fig 4.5 ESR spectrum of solution a

Fig 4.5 shows the spectrum obtained from the solution containing $MnCl_2$ only, and confirms that Mn^{2+} is present as an octahedral complex (with six water molecules). The manganese coupling constant obtained from this spectrum is ~90G (= 90mT). A good approximation to the coupling constant can be made by measuring the distance between two adjacent peaks (although for technical reasons it is easier to measure the spacing between the outer lines and then divide by 5).

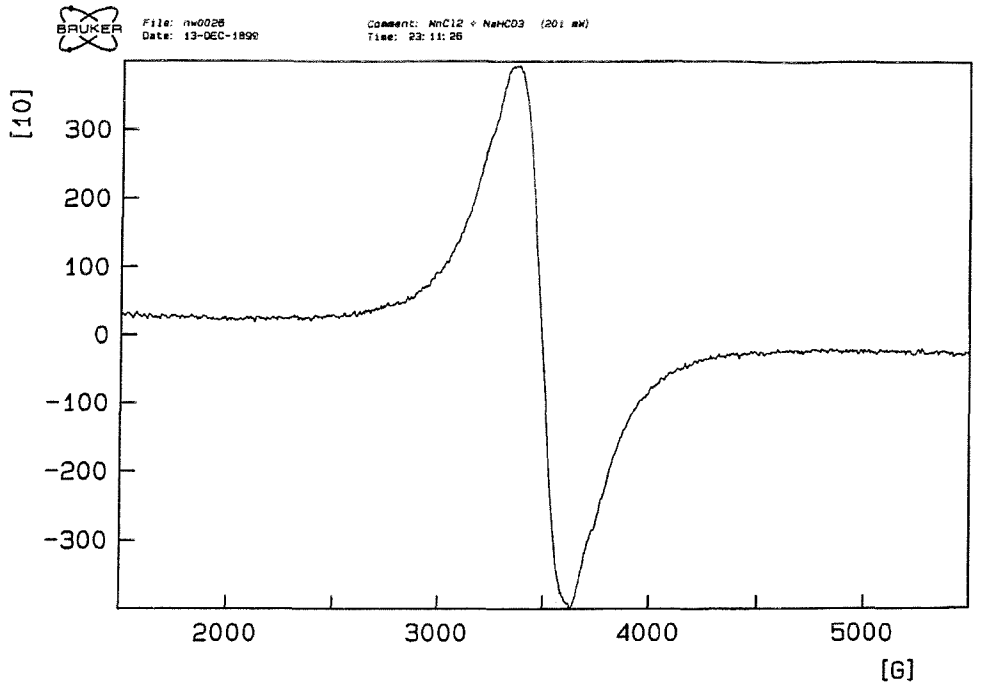

Fig 4.6 ESR spectrum of solution d

Fig 4.6 shows the spectrum obtained from the solution containing $MnCl_2$ and $NaHCO_3$. When first mixed this solution produced a white precipitate in suspension ($MnCO_3$), the spectrum shown was produced from the freshly mixed solution and hence contained suspended $MnCO_3$. When this solution was filtered through a 0.45μm Nylon syringe filter, no signal was observed from the filtrate (spectrum not shown). This suggests that, at the concentrations used, all the Mn^{2+} present reacts with the bicarbonate. This spectrum consists of a single peak (linewidth ~ 350G). The loss of the hyperfine structure is consistent with the loss of symmetry (displacement of H_2O by HCO_3^-) of the $Mn^{2+}(6H_2O)$ ion as it reacts to give $MnCO_3$. The increase in linewidth in this spectrum compared with that for the spectrum of $MnCl_2$ indicates a reduction in the spin lattice relaxation time of manganese.

Fig 4.7 shows the spectrum obtained for solution e. ($MnCl_2$ and Na_2EDTA). It can be seen that the intensity of the signal has been reduced compared to that for the $MnCl_2$ solution alone. To obtain a more accurate determination of the amount of $MnCl_2$ that has reacted we would need to integrate the signal and determine the peak areas. In addition, the manganese coupling constant appears to have increased slightly from

~90G to ~110G. Again, this is consistent with a reduction in concentration of the $Mn^{2+}(6H_2O)$ ion and the displacement of H_2O by the EDTA ligand (with a corresponding loss of symmetry of the molecule).

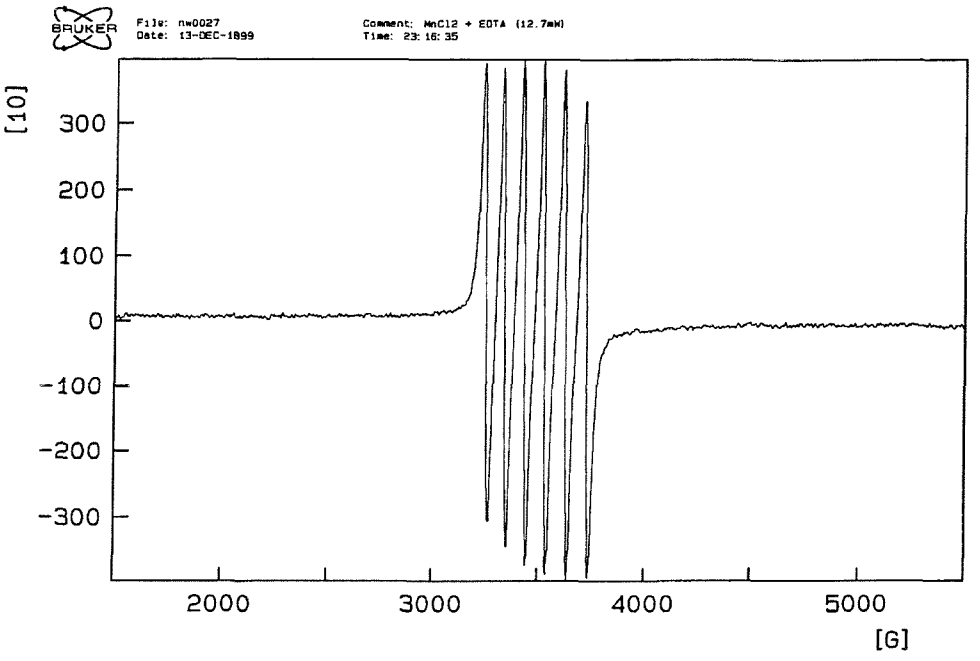

Fig 4.7 ESR spectrum of solution e

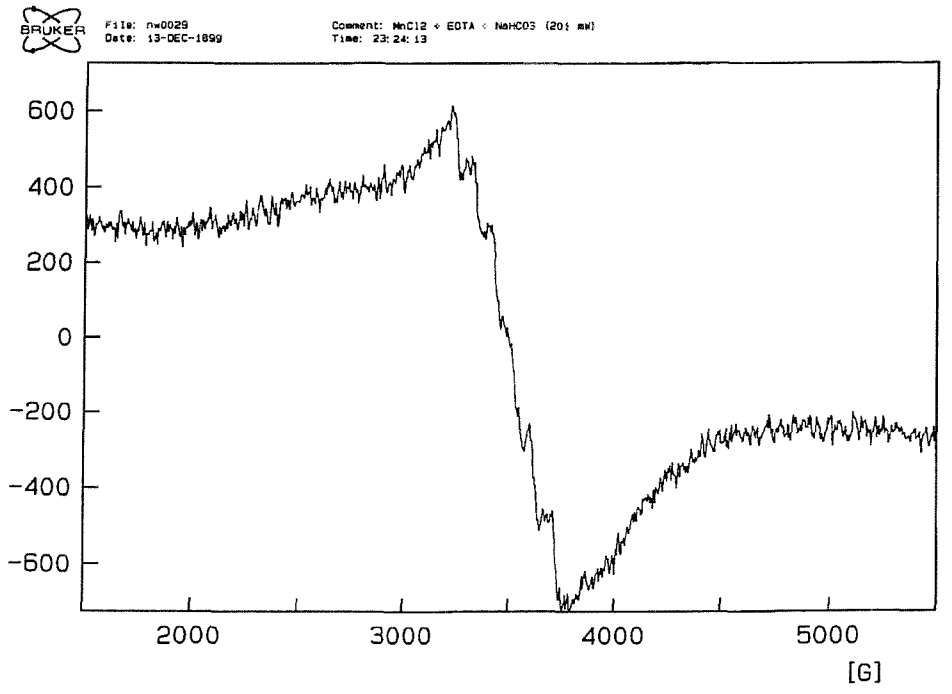

Fig 4.8 ESR spectrum of solution f

Solution f (Fig 4.8) gave a very weak, broad signal, that may be indicative of two superimposed peaks (some evidence of hyperfine structure can still be seen and may be due to unreacted Mn^{2+}). The linewidth of this signal, as for $MnCO_3$, is about 350G, although the lineshape for these signals are different and may indicate the presence of more than one line.

A solution of disodium manganese EDTA ($Na_2MnEDTA$)was prepared at 0.5%w/w in water and diluted 1:10. This solution was analysed as before, and gave a spectrum simillar to that of solution f (Fig. 4.9).

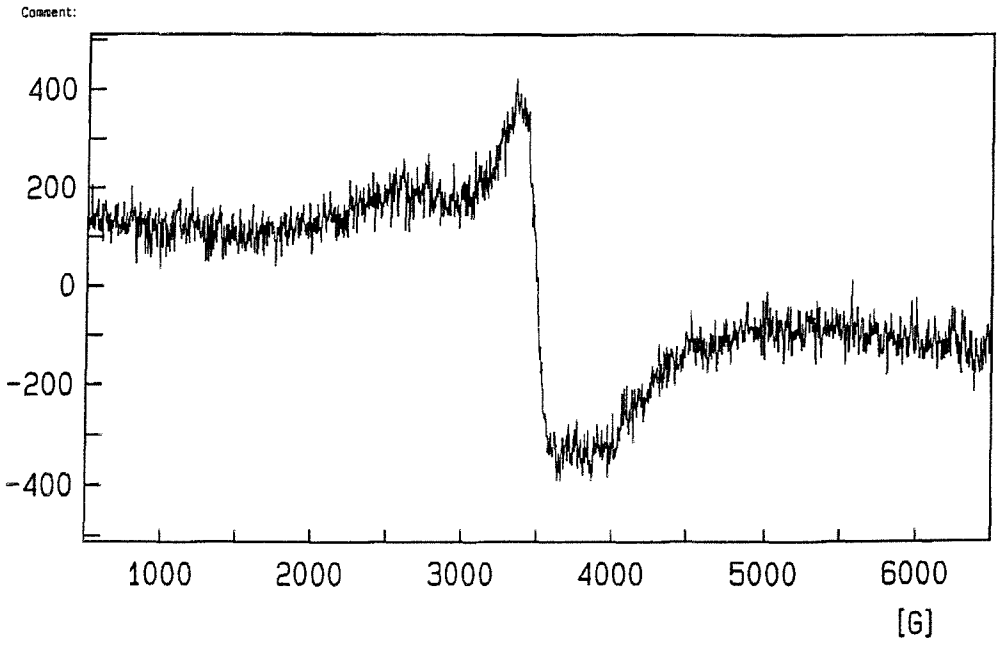

Fig. 4.9. *ESR spectrum of dilute* $Na_2MnEDTA$ *solution (0.05%w/w in water)*

To confirm the spectrum of $Na_2MnEDTA$ the more concentrated solution (0.5% w/w) was analysed, this gave the spectrum as shown in fig. 4.10. This spectrum gives a better signal/noise ratio (thus the detail of the spectrum is more easily observed) and demonstrates the existance of two superimposed signals. This indicates the possibility that $Na_2MnEDTA$ may exist, in solution, as two distinct species.

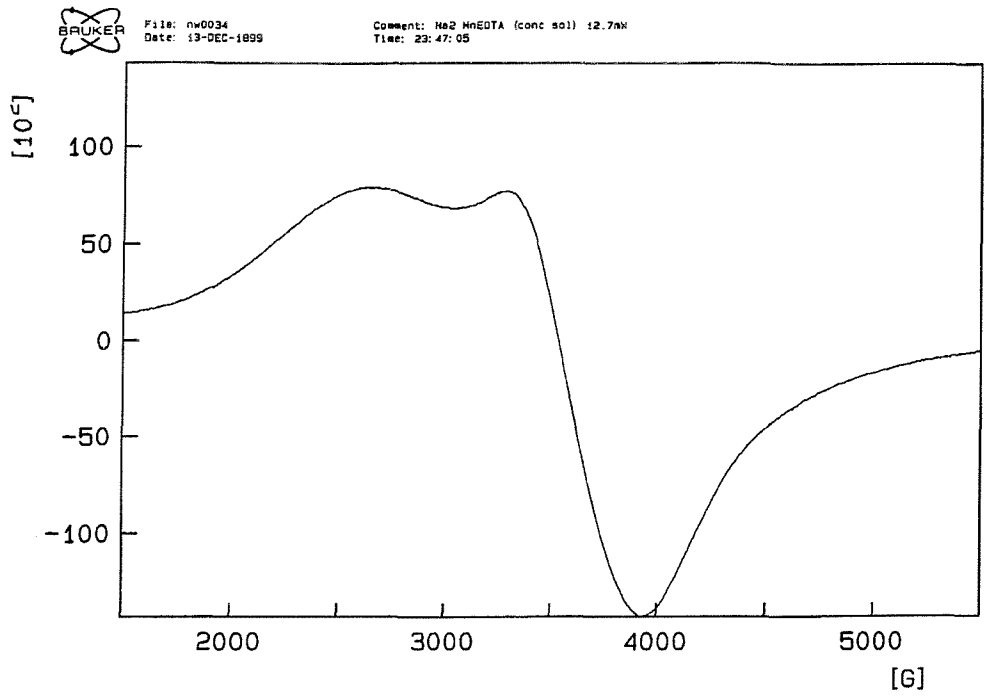

Fig. 4.10. ESR spectrum of $Na_2MnEDTA$ at 0.5% w/w in water.

Fig. 4.11 represents the structure of $Na_2MnEDTA$. Usually one would expect the nitrogen atoms and all four O^- atoms to be bound to the manganese in an octahedral

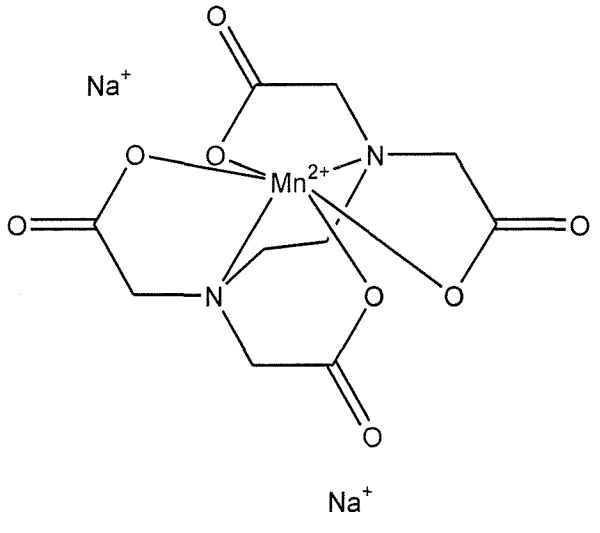

Fig. 4.11 Structure of $Na_2MnEDTA$

configuration; however it is possible that in solution one or more of the O^- (bound to manganese) groups may be dissociated from the manganese, and are ionically bonded to the sodium ions. It is therefore possible that there is the equilibrium

$$Na_2MnEDTA \leftrightarrow (MnEDTA)^{2-} + 2Na^+$$

To see if this equilibrium is feasible we need to examine the dissociation constants for EDTA.

The pKa values for H_4EDTA have been reported as [4, 5]:

pKa_1 1.99

pKa_2 2.67

pKa_3 6.16

pKa_4 10.26

and as the pH of a 0.5% w/w solution of $Na_2MnEDTA$ in water is about 6.9 then at least two of the acetic acid groups are fully ionised as the acetate, and the third partially ionised. These data support the proposed equilibrium.

To test this proposal further, it should be possible to observe a change in the spectrum of $Na_2MnEDTA$ by adding excess sodium ions to the solution and so force the equilibrium to the left. To do this a solution of $Na_2MnEDTA$ was prepared in water containing a tenfold molar excess of sodium chloride and its ESR spectrum recorded. The resulting spectrum (Fig. 4.12) was compared with the spectrum of $Na_2MnEDTA$ recorded previously (Fig. 4.10).

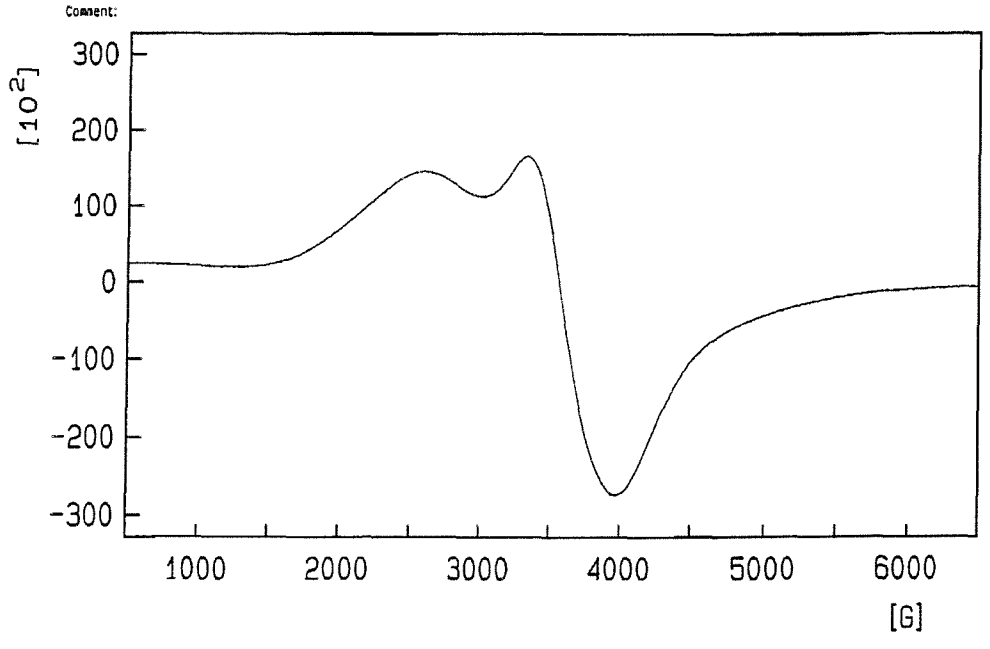

Fig. 4.12 ESR spectrum of $Na_2MnEDTA$ (0.5%w/w) with 10x molar excess NaCl

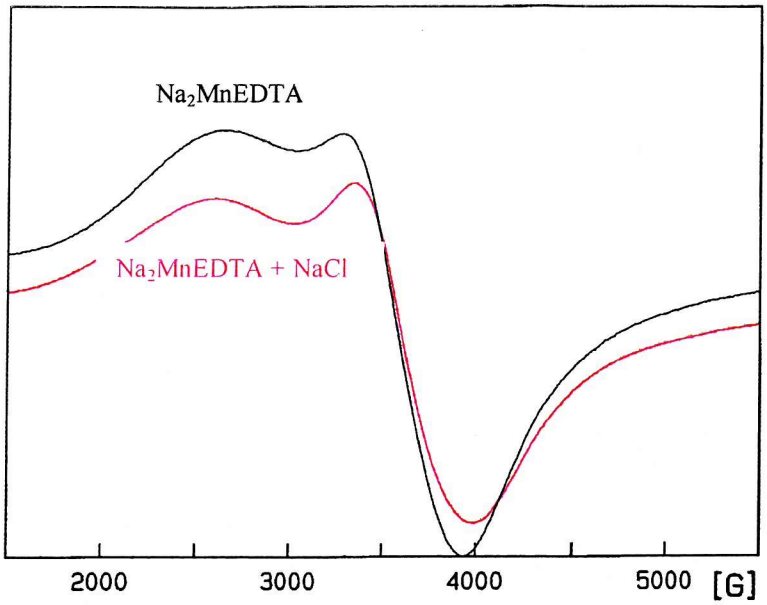

Fig. 4.13. Overlay of spectra from Fig. 4.10 and 4.12

These spectra show that, although there is no change in the overall shape of the spectra, there appears to be a slight change in relative intensities of the two peaks observed, with the width of the lines remaining unchanged.

The spectra observed for $Na_2MnEDTA$ can be shown to consist of two peaks by simulating the spectra obtained. The absorption curve obtained for ESR spectroscopy is of the Lorentzian form where:

$$I_{(B)} \propto \frac{w}{4(B_{max} - B)^2 + w^2}$$

and $I_{(B)}$ = intensity of the signal at field value B, w = peak width and B_{max} = peak centre.

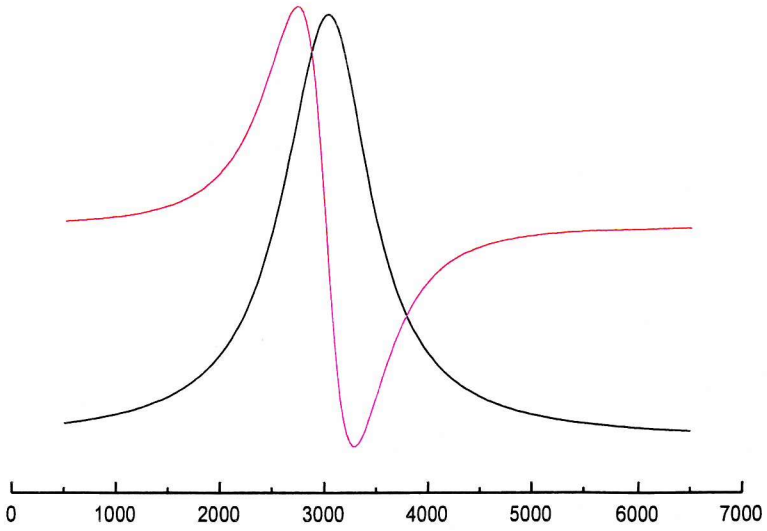

Fig. 4.14 Lorentzian curve and 1st derivative of a peak centred at 3000G and with a width of 1000G

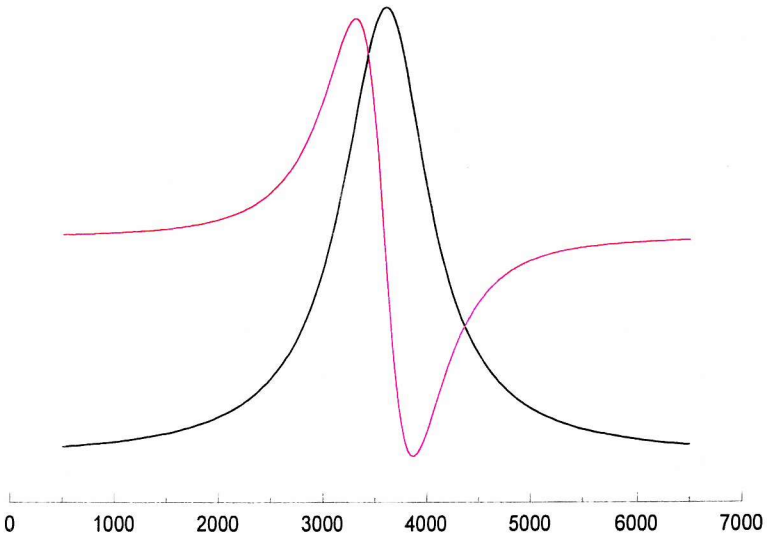

Fig. 4.15 Lorentzian curve and 1st derivative of a peak centred at 3850G and with a width of 1000G

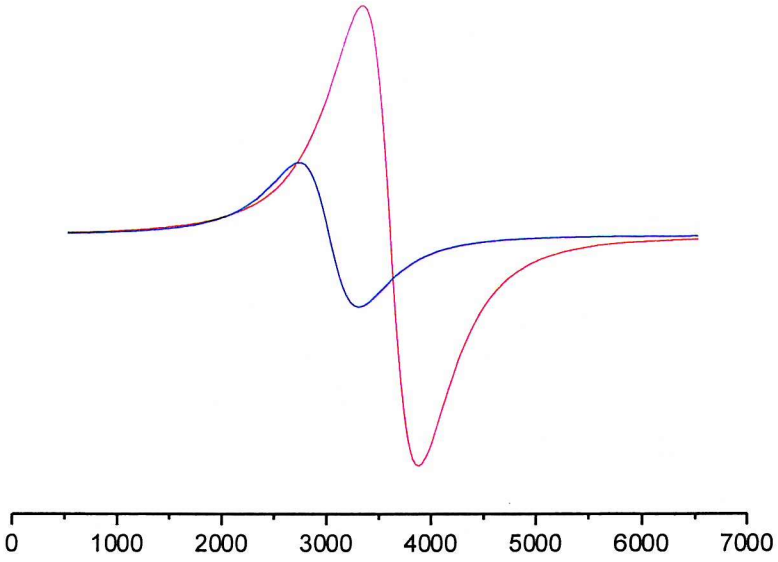

Fig. 4.16 Overlay of 1st derivative curves of Figs. 4.14 and 4.15

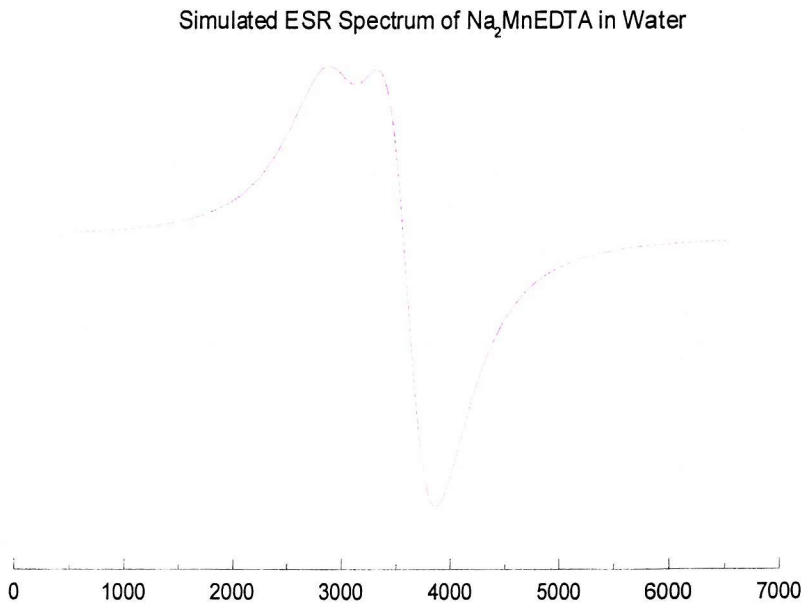

Fig. 4.17 Sum of 1st derivative curves

Figures 4.14 to 4.17 show that the shape of the simulated spectrum obtained for disodium manganese EDTA is consistent with a signal produced by two distinct peaks (both with a peak width of 1000G). This compares favourably with the actual spectrum obtained for disodium manganese EDTA (Figs. 4.10 and 4.12). From the simulated spectra, we can calculate the g factor for both of the signals (using equation 3) as approximately 2.26 and 1.76 compared to a g factor of 1.93 for Mn^{2+} in solution. These changes in the g factor reflect changes in the spin-orbit coupling.

Analysis of Pseudocatalase cream samples.

To check whether there are any differences in the chemistry involved between the solution samples, analysed previously and Psuedocatalase cream samples it was necessary to examine the ESR spectra for manganese in the presence of the cream vehicle.

The following samples of Pseudocatalase cream were prepared for analysis by ESR

a. Full product – containing cream base, manganese chloride, disodium EDTA and sodium bicarbonate.
b. Full product (as above) – centrifuged at 5000 rpm for 10 minutes
c. Cream base with sodium bicarbonate only
d. As c. with manganese chloride
e. As c. with disodium EDTA

The samples were placed directly in the flat cell and the spectra recorded – the cell was washed as described previously between analyses. Figs 4.18 to 4.20 show the spectra obtained.

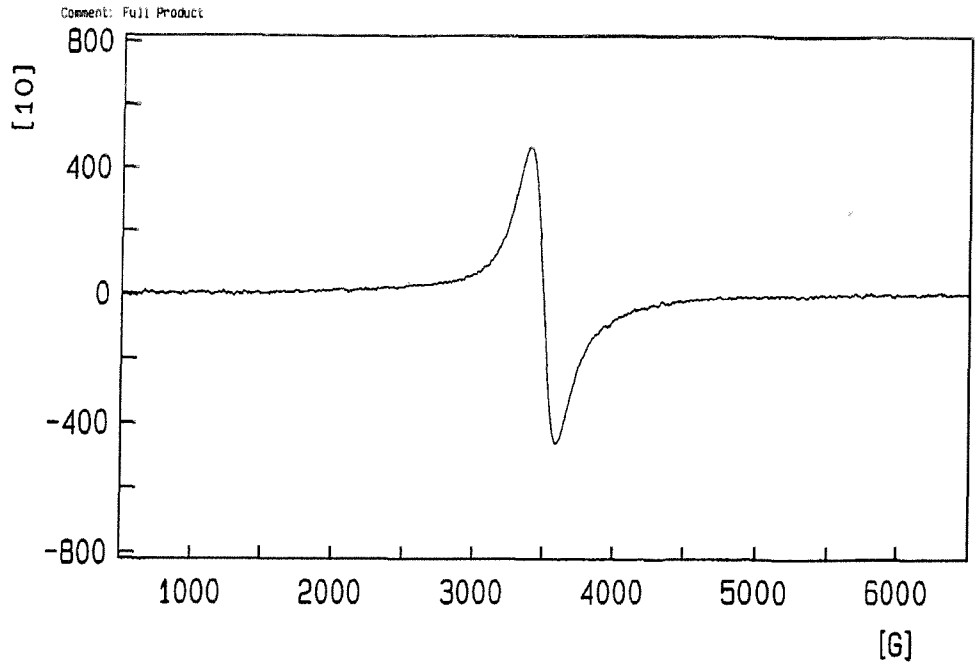

Fig 4.18 ESR spectrum of sample a. Pseudocatalase cream – full product

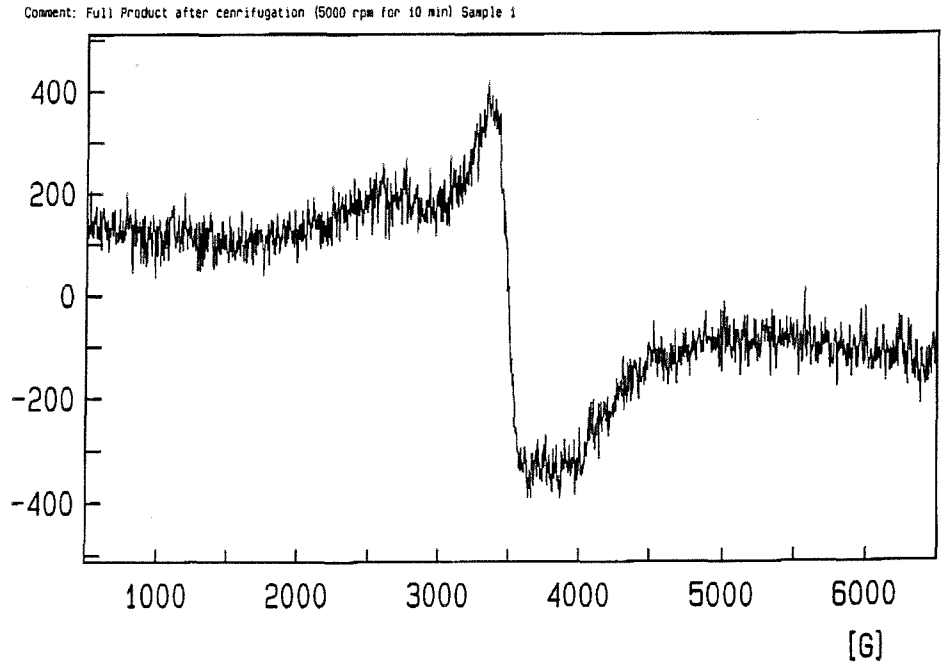

Fig. 4.19 ESR spectrum of sample b. Pseudocatalase cream – full product after centrifugation.

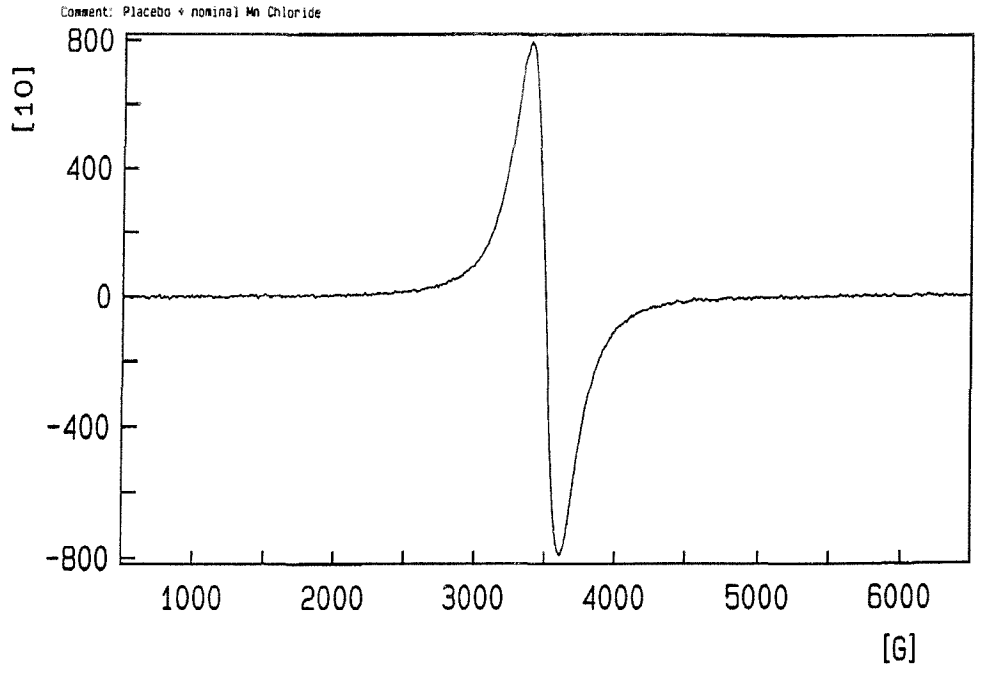

Fig. 4.20 ESR spectrum of sample d. – cream base with manganese chloride and sodium bicarbonate

Spectra for samples c. and e. are not shown as no peaks were seen in these samples. Samples a. and d. gave spectra that are consistent with the presence of a suspension of solid $MnCO_3$ in the samples. Although the signal intensity is reduced for the full product, this is due to manganese chelating with the EDTA in the sample (Figs. 4.18 and 4.20).

As the cream samples are extremely viscous it is not possible to filter them to remove any of the particulate $MnCO_3$, as was done for the aqueous solutions, however it was possible to centrifuge the sample, and analyse the cream. This was performed by placing a sample of the cream (b) in a centrifuge tube, and spinning the sample at 5000 rpm for 10 minutes. The sample was then removed without disturbing the precipitated $MnCO_3$ and its ESR spectrum measured (Fig. 4.19). The resulting spectrum demonstrates features consistent with the spectra obtained for $Na_2MnEDTA$ (Fig. 4.9).

4.3 Discussion

It is apparent that the ESR technique does not give as much information as expected, mainly because of the large linewidths of the single lines obtained from the majority of the systems studied. Nevertheless, some information can be drawn from the results of this study.

The narrow line associated with manganese carbonate is appears to be consistent with manganese ions in close proximity.

The presence of two superimposed peaks in the manganese EDTA system with bicarbonate gives a signal which could be associated with a bicarbonate bridged dimer; although it is not clear (from these spectra) if the two manganese ions are chelated by EDTA or not.

The low symmetry of these complexes appears to generate a large zero-field splitting, hence the broad lines observed. For systems with more than one unpaired electron ($S>1/2$) the ground state can be split in the absence of an external magnetic field due to the local site symmetry – the zero-field splitting. For odd-electron systems this results in pairs of energy levels known as Kramer's doublets. The observed ESR spectrum may contain transitions within each of the ground-state Kramer's doublets. There are two important conditions under which it may not be possible to observe an ESR signal, even when unpaired electrons are present:

1. If the system has an even number of unpaired electrons then the zero-field splitting within the ground state may result in the ESR transitions being undetectable.
2. If the paramagnetic centres occur in pairs then coupling of the individual spins may result in the ESR signal being undetectable or even absent, although the individual centres may have an odd number of unpaired electrons.

However, it may be possible to obtain further information by freezing the solutions and recording the ESR spectra at low temperatures (close to those of liquid nitrogen or liquid helium).

An interesting article [6] seems to indicate that an oxo-bridged MnEDTA dimer may exist, albeit as an unstable intermediate. In this paper, Hage and co-workers demonstrated that oxo-bridged Mn complexes act as very effective bleaching agents by catalysing the oxidation of polyphenolic substrates by hydrogen peroxide. Their

data suggests that upon the addition of a substrate the manganese ions are taken to a mixed valance state; this was characterised by ESR spectroscopy at 77K.

Additional information to support the formation of binuclear, μ-dihydroxo EDTA complexes (Fig. 4.21) can be found in references [7-9]. These papers also indicate that, in solution the μ-dihydroxo complex exists in part as a dehydrated μ-oxo dimer and that this is in equilibrium with the monomeric form.

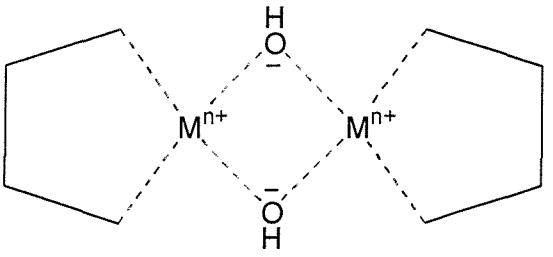

Fig. 4.21 A μ-dihydroxo binuclear metal chelate

It has also been shown [10, 11] that binuclear Fe complexes with a triply bridged (μ-dicarboxylate-μ-oxo) can be synthesised. These complexes are of the type $[LM^{n+}(RCOO^{-})_2O^{2-}M^{n+}L]^{2+}$ and several analogues of this type have been prepared replacing the acetato bridges with formate and benzoate. It has been reported that similar complexes have been prepared using Mn^{3+} [12, 13]. These metal ions are highly charged and strongly hydrolysed in aqueous solution. These two properties, while interrelated, are both needed to provide the coulombic forces necessary to hold the unit together, as well as to polarise water sufficiently to dissociate the two hydrogen ions required to produce the oxo bridge (although the latter may be aided by the presence of peroxide and excess bicarbonate).

A complementary approach, which may be used, is to look at the possible radical formation of the dye alizarin. It is probable that the oxidation of the dye is not a single step reaction and that a radical will be formed during this process. Unfortunately, time did not permit any further exploration along this avenue, but this could be forwarded as part of a separate research programme.

References

1. A. Carrington and A. D. McLachlan, Introduction to Magnetic Resonance, Chapman & Hall, 1983.
2. J. E. Wertz and J. R. Boulton, Electron Spin Resonance: Elementary Theory and Practical Applications, Chapman & Hall, 1986.
3. C. N. Banwell and E. M. McCash, Fundamentals of Molecular Spectroscapy, 4th ed., McGraw-Hill Book Company Europe, 1994.
4. CRC Handbook of Organic Analytical Reagents (K L Cheng, K Ueno, T Imamura, eds.), CRC Press, Boca Raton, 1982.
5. R. M. C. Dawson, D. C. Elliot, W. H. Elliot, K. M. Jones, Data for Biochemical Research, 3rd ed., Clarendon Press, Oxford, 1986.
6. R. Hage, J. E. Ilburg, J. Kerschner, J. H. Koek, E. L. M. Lempers, R. J. Martens, U. S. Racheria, S. W. Russell, T. Swartoff, M. R. P. van Vliet, J. B. Warnaar, L. van der Wolf and B. Krijnen. *Nature.*, **369**, 637, 1994.
7. G. L. Gustafson and A. E. Martell, *J. Phys. Chem.*, **67**, 576, 1963.
8. S. J. Lippard, H. J. Schugar and D. Walling, *Inorg. Chem.*, **6**, 1825, 1967.
9. G. McLendon, R. J. Motekaitis and A. E. Martell, *Inorg. Chem.*, **15**, 2306, 1976.
10. W. H. Armstrong and S. J Lippard, *J. Am. Chem. Soc.*, **105**, 4837, 1983.
11. K. Wieghardt, K. Pohl and W. Gerbert, *Agnew. Chem.*, **95**, 729, 1983.
12. K. Wieghardt, U. Bossek, D. Ventur and J. Weiss, *J. Chem. Soc. Chem. Commun.*, 347, 1985.
13. J. E. Sheats, R. S. Czernuszewicz, G. C. Dismukes, A. L. Rheigold, V. Petrouleas, J. Stubbe, W. H. Armstrong, R. H. Beer and S. J. Lippard, *J. Am. Chem. Soc.*, **109**, 1435, 1987.

Conclusions

A number of techniques have been employed during the course of this research to detect and identify the active species in Pseudocatalase, including ESR spectroscopy and capillary electrophoresis. So far, all that has been seen is the presence of $Mn^{II}EDTA$ and $MnCO_3$. Additionally if a manganese-EDTA-bicarbonate complex does exist it would appear to be transparent to the techniques used so far. It is questionable whether there is a reaction product from $Mn^{II}EDTA$ and bicarbonate, as bicarbonate is a very weak ligand, the credibility of bicarbonate ions displacing other groupings within the EDTA complex is open to question.

The recent discovery that the relationship between the catalytic activity and the concentration of $Mn^{II}EDTA$ was not linear but proportional to the square of the concentration has given additional insight into the mechanism.

A series of Pseudocatalase creams were manufactured containing a range of manganese chloride concentrations (the amount of bicarbonate and EDTA were kept constant at 2.3% and 0.5% respectively). The cream samples were analysed for catalytic activity (using alizarin as a substrate) and $Mn^{II}EDTA$ content using the methods described in chapters 2 and 3. The results are shown below.

% nominal $MnCl_2$ concentration in Pseudocatalase	Rate x 10^{-5} $AU.s^{-1}$	Concentration of MnEDTA (as mmol Mn)	$[mmol\ Mn]^2$
10	21	0.133	0.018
20	79	0.205	0.042
40	145	0.377	0.142
50	166	0.477	0.227
60	219	0.576	0.332
70	488	0.905	0.819
80	860	1.224	1.498
100	864	1.233	1.520
120	829	1.206	1.454
150	889	1.245	1.550

From this data, it can be seen that both the catalytic activity and the amount of MnEDTA formed reach a plateau, as would normally be expected, at a manganese level of about 1.5mmol, after which any excess manganese would be precipitated as the carbonate.

A plot of the rate of oxidation of alizarin against the square of the amount of MnEDTA found in the samples gave the graph shown in Fig. 5.1

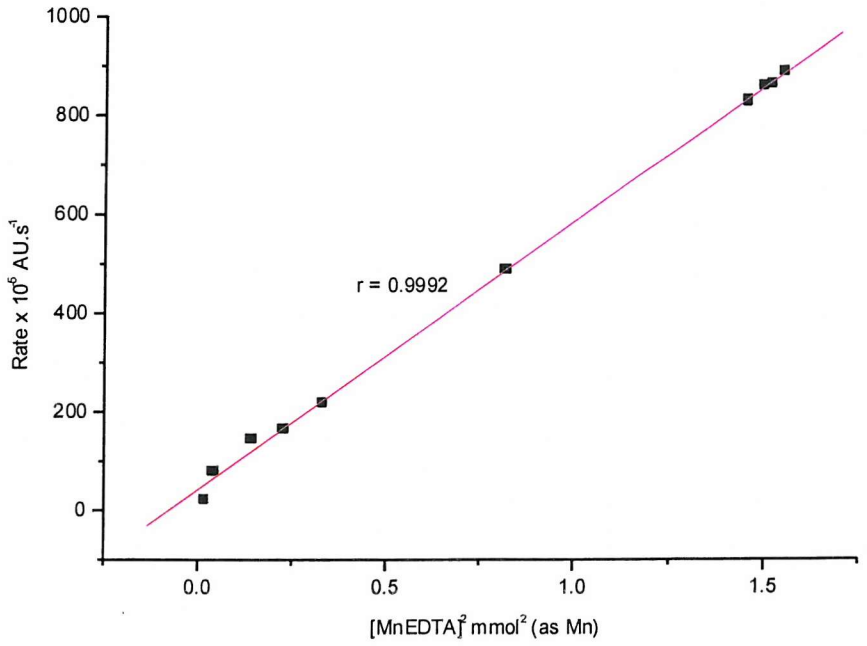

Fig. 5.1 Plot of catalytic activity vs. amount of MnEDTA.

This would imply that two molecules of MnEDTA are involved in the active species. It is difficult to envisage how a poor ligand like bicarbonate can bind two MnEDTA molecules together. This leads to the suspicion that the oxidising agent (in this case hydrogen peroxide) is involved in some way. It is possible that a bi-nuclear manganese complex could be formed by oxidation, with bicarbonate groups forming the bridging ligands (see Fig. 5.2)

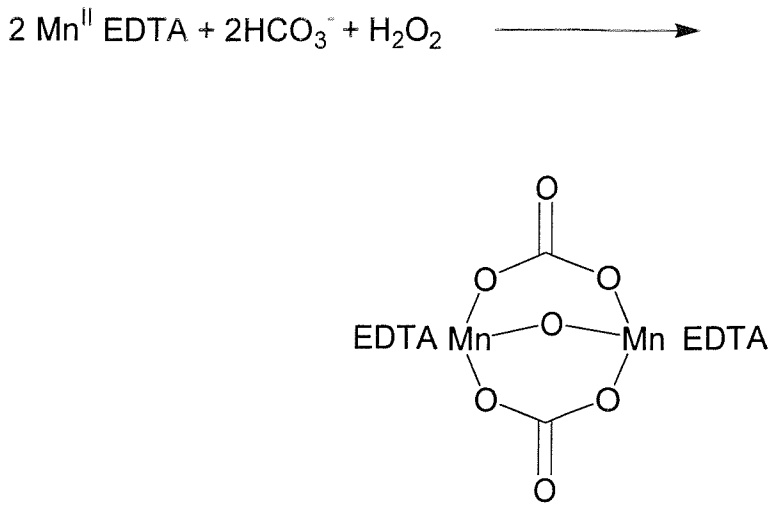

Fig. 5.2 Possible formation of a bi-nuclear Mn complex.

Computer generated models (based on both molecular mechanical methods, MM2, and semi-empirical methods, MOPAC) of this structure indicate that such a complex would be, structurally, relatively stable (minimum steric energy is about –550kcal), but more importantly it would have two interesting properties.

1. The oxidation state preferred by both manganese atoms would be 3.
2. The Mn-Mn spatial separation would be around 3.3 Å, and could cause partial single bond formation by extensive d-orbital overlap.

These two factors would produce a bi-nuclear complex with unusual features. Resonance structures are possible that allow multi-valency states (Fig. 5.3).

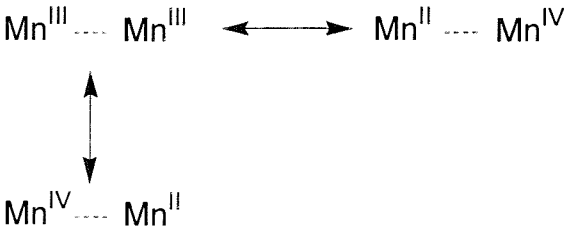

Fig. 5.3. Resonance structures of Mn^{III}-Mn^{III}.

This would mean that such a bi-nuclear complex would have one manganese atom at valency 4, allowing it to behave as a strong oxidising agent. This type of bi-nuclear, multi-valence structure has strong biological significance as many metallo-proteins contain a bi-metallic centre, such as Hemerythrin, Ribonucleotide reductase, Purple

acid phosphatase (all containing Fe-Fe centres) and Hemocyanin, Tyrosinase, Cytochrome *c* oxidase (containing Cu-Cu centres).

The proposed complex has very similar structural features to the bi-nuclear multi-valency manganese complexes studied by Hage *et al.* [1], some of which are shown in Fig. 5.4. These compounds were evaluated as detergent additives for oxidising clothing stains, i.e. a similar mode of action to Pseudocatalase.

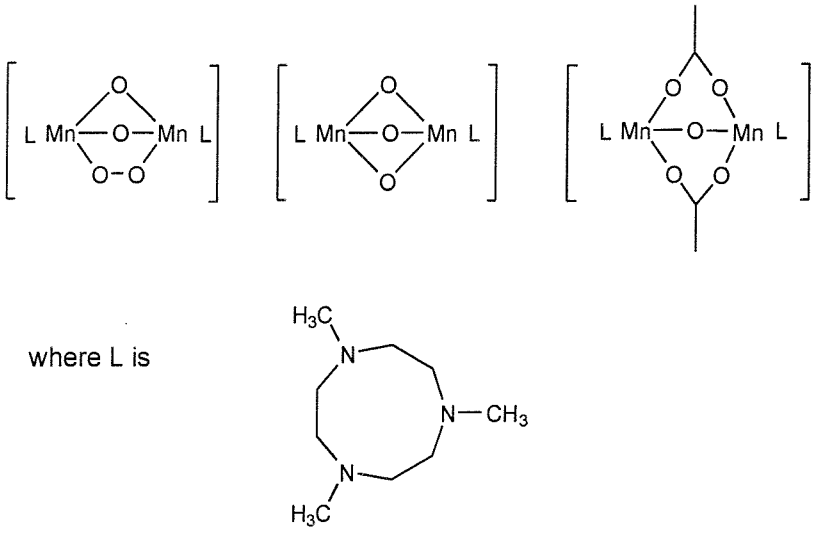

Fig 5.4. Some binuclear Mn complexes investigated as bleaching agents [1].

Perhaps the unique features of Pseudocatalase activity are due to the unique redox potentials of such bi-nuclear complexes.

$$Mn^{II} - Mn^{IV} + \text{Substrate} \longrightarrow Mn^{II} - Mn^{II} + \text{oxidised Substrate}$$

Or more specifically:

$$Mn^{II} - Mn^{IV} + \text{DOPA} \longrightarrow Mn^{II} - Mn^{II} + \text{DOPA quinone}$$

It is likely that on reduction to Mn^{II}-Mn^{II} the bi-nuclear complex will breakdown to regenerate Mn^{II}EDTA and bicarbonate ions, thus allowing the cycle to begin again by reaction with more hydrogen peroxide. Only two steps would be required for the whole process (Fig 5.5).

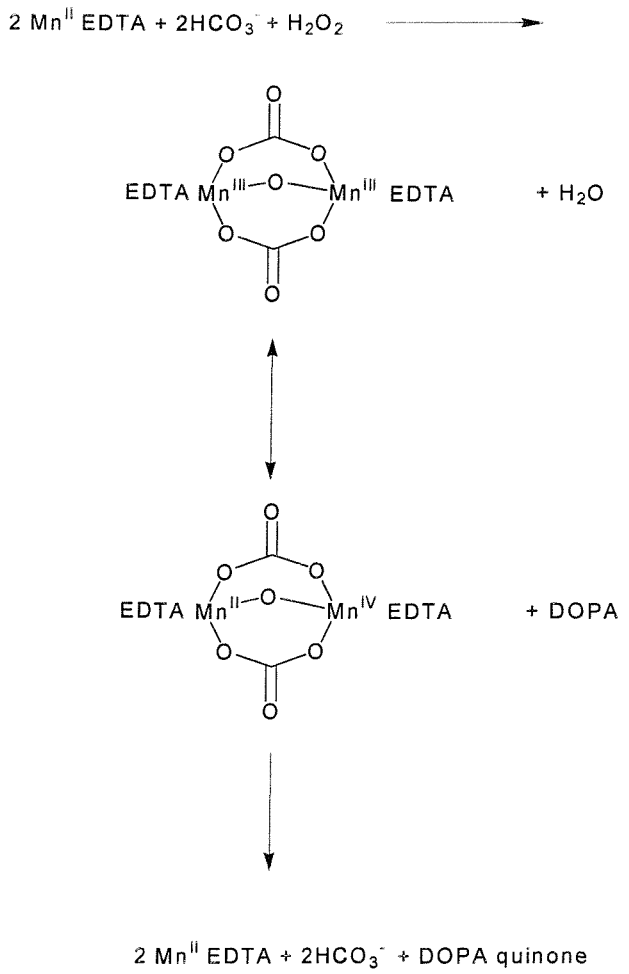

Overall:

$$DOPA + H_2O_2 \rightarrow DOPA\ quinone + H_2O$$

Fig. 5.5. Proposed reaction scheme for the oxidation of DOPA to DOPA quinone by Pseudocatalase.

If this is correct and such a bi-nuclear manganese complex is formed, then which species is the catalyst? The bi-nuclear species cannot by definition be described as such as it is clearly a reaction intermediate. Therefore, there is only one possible candidate as catalyst and that is Mn^{II}EDTA. If this is so then this research has been completed successfully, the active has been identified, and a method developed for its quantitative analysis in Pseudocatalase cream.

Further work would be required to confirm this proposition. It may be possible to monitor the changing oxidation states of manganese during the reaction process (by ESR at low temperatures) or by measuring the amount of Mn^{II}EDTA present at

different stages during the reaction. If $Mn^{II}EDTA$ is acting as a true catalyst, then its concentration will remain unchanged, both at the start and at the end of the reaction.

References

1. R. Hage, J. E. Ilburg, J. Kerschner, J. H. Koek, E. L. M. Lempers, R. J. Martens, U. S. Racheria, S. W. Russell, T. Swartoff, M. R. P. van Vliet, J. B. Warnaar, L. van der Wolf and B. Krijnen. *Nature.*, **369**, 637, 1994.